AD-A156 829 A COMPARISON OF SWEPT FREQUENCY AND FFT METHODS USED TO 1/1
CALIBRATE ARRAY TEST MODULES(U) WEAPONS SYSTEMS
RESEARCH LAB ADELAIDE (AUSTRALIA) G B GILLMAN OCT 84
UNCLASSIFIED WSRL-0383-TR F/G 20/1 NL

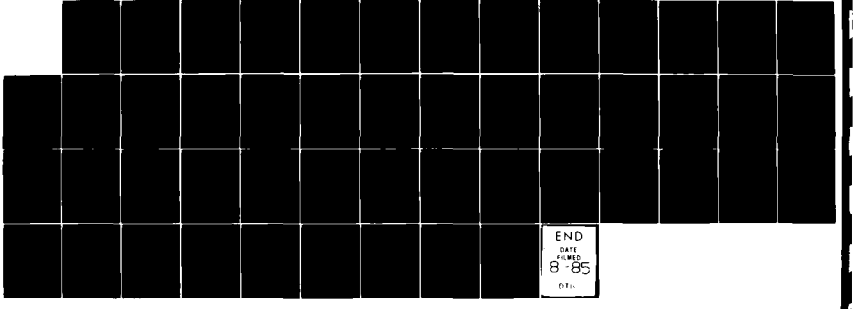

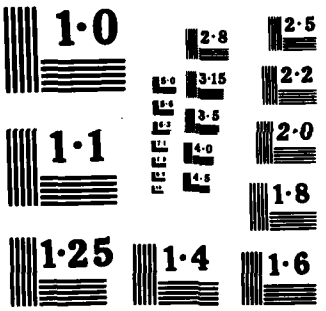
1·0
1·1
1·25
1·4
1·6
1·8
2·0
2·2
2·5
2·8
3·15
3·5
4·0
4·5

WSRL-0383-TR

AR-004-117

DEPARTMENT OF DEFENCE

DEFENCE SCIENCE AND TECHNOLOGY ORGANISATION

WEAPONS SYSTEMS RESEARCH LABORATORY

DEFENCE RESEARCH CENTRE SALISBURY
SOUTH AUSTRALIA

TECHNICAL REPORT
WSRL-0383-TR

A COMPARISON OF SWEPT FREQUENCY AND FFT METHODS USED TO CALIBRATE ARRAY TEST MODULES

G.B. GILLMAN

Approved for Public Release

OCTOBER 1984

COPY No. 30

AR-004-117

DEPARTMENT OF DEFENCE

DEFENCE SCIENCE AND TECHNOLOGY ORGANISATION

WEAPONS SYSTEMS RESEARCH LABORATORY

TECHNICAL REPORT

WSRL-0383-TR

A COMPARISON OF SWEPT FREQUENCY AND FFT METHODS USED TO CALIBRATE ARRAY TEST MODULES

G.B. Gillman

S U M M A R Y

A description is given of swept frequency and FFT methods used to calibrate array test modules. The FFT method is shown to give sensitivity versus frequency plots with relative ease and known accuracy. The swept frequency method is capable of giving similar results but only after operator interpretation of the mean of fluctuating signals and calculations on a point to point basis. A digital filtering method is briefly described which can be used to process the signals obtained in swept frequency calibration obviating the need for operator interpretation. The accuracy of the FFT method is discussed and an overall accuracy figure is obtained for the derived sensitivity of the test array. A summary of the FFT method is given as a guide for future hydrophone calibration experiments.

POSTAL ADDRESS: Director, Weapons Systems Research Laboratory, Box 2151, GPO, Adelaide, South Australia, 5001.

TABLE OF CONTENTS

LIST OF FIGURES

3. (a) The reference and unknown hydrophone measurement system. The analyser measures the transfer function between A and B. (b) A simplified version of (a)

4. The filter passband shapes for Flat Top, Hanning and Uniform functions. Δf is the filter spacing between the Nth and (N+1)th filter frequency

5. A typical digitised swept frequency calibration plot. The upper curve is the reference hydrophone output and the lower is the array output. The vertical scale represents a relative response

6. A plot of the overall sensitivity and amplifier gain for array AM13. The hydrophone sensitivity S is equal to overall sensitivity minus amplifier gain and is tabulated for 100 Hz

7. A plot of the sensitivity difference between the reference and an unknown hydrophone. The plot is derived from the two response curves plotted in figure 3

8. A plot of the first 25 frequency bins of the normalised Fourier spectrum of the difference curve of figure 5 and a window of width 44 bins

9. The smoothed difference curve resulting from the multiplication in frequency space of the original difference curve and window spectra and applying the inverse Fourier transform

10. A plot of the sensitivity in dB re 1 V/µPa versus frequency for array AM11. Each hydrophone group is indicated

11. A plot of the sensitivity in dB re 1 V/µPa versus frequency for array AM12. Each hydrophone group is indicated

12. A plot of the sensitivity in dB re 1 V/µPa versus frequency for array AM13. Each hydrophone group is indicated

13. A plot of the sensitivity in dB re 1 V/µPa versus frequency for array AUSTAM. Each hydrophone group is indicated. The curve for the capacitor should be decreased by a further 40 dB

14. Plots of the coherence (top set of traces) and transfer function amplitude for the TEAC tape recorder channel 1 between the play and replay channels for various recording levels as indicated

15. A plot of the transfer function of the signal amplifier used to amplify the signal prior to tape recording. The gain is switched to 0 dB, the gain is within ±0.2 dB at other settings and is an identical shape

16. The transfer function between record and replay, channels 1 and 2 at $3\frac{3}{4}$ ips and $7\frac{1}{2}$ ips tape speeds using TDK AD120 tape

17. The transfer function between channels 1 and 2 after pseudo-random noise was recorded via one machine and played back on another. The magnitude is indicated by a dotted line

18. The transfer function between channels 1 and 7 after pseudo-random noise was recorded via one machine and played back on another

19. An example of the cross calibration of two hydrophones using the swept frequency method. Only relative signal levels are shown

20. The difference in sensitivity between the two hydrophones plotted on a logarithmic frequency scale. Absolute levels are shown

21. The difference in sensitivity between the two hydrophones plotted on a linear frequency scale. Absolute levels are shown. Note the periodic nature of the fluctuations

22. The normalised spectrum of a rectangular window and the difference curve. The window width is chosen so that its minima coincides with some of the higher frequency components

23. The reconstituted curve after smoothing with the window shown in figure 20

1. BACKGROUND

A number of calibration experiments have been performed in the past to derive the sensitivity of hydrophone groups in a number of the MSC test arrays. Most of the experiments used the swept frequency method of calibration. Following some trial results some doubts were raised as to the derived sensitivity figures. A brief calibration check was attempted using FFT techniques and the results did not confirm the earlier work. Sensitivity figures were then calculated from the trial acoustic records by cross comparison of submarine radiated noise and array flow noise with the estimated sensitivity of a particular hydrophone assembly. These figures were approximately the same as the FFT derived ones and thus a further set of calibration experiments was implemented to finalise the discrepancies.

It was decided to concentrate on the FFT method as it was easy to control and quantify most of the variables involved in a calibration experiment. In particular, the measurement of the signal coherence enables the operator to check the validity of the measurement. Particular care was taken to check all aspects of the calibration procedure, in this way it was hoped to calculate the uncertainty limits on the final derived sensitivity figures.

The swept frequency method was also used to calibrate one of the test assemblies and a direct comparison between the two techniques was made. Based on these experiments a recommended calibration procedure was produced which can be used as the basis of future calibration experiments.

2. CALIBRATION METHODS

Both the swept frequency and FFT calibration methods are based on the measurement of the relative response between a known reference hydrophone and the unknown when subject to exactly the same acoustic field. In theory the reference hydrophone first measures the acoustic field and the hydrophone is then replaced by the unknown to ensure that the measurements are performed in the same acoustic field. In practice with a frequency range of 20 Hz to 1.6 kHz, the acoustic field is sufficiently uniform to permit simultaneous measurement of both hydrophone outputs when they are close to each other and about a metre from the acoustic source. The differences in the methods relate to the nature of the acoustic source signal and the analysis of the received signals.

2.1 Swept frequency

In this method the acoustic source frequency is swept (usually at a logarithmic rate) over the frequency range of interest. The rate is low enough so that no significant frequency shift occurs and so that there is time for the acoustic field to be established if strong multipath interference is a problem. The measurement then approximates to steady state conditions at any frequency. The hydrophone signal is detected by an RMS level detector and the signal level is usually recorded on chart paper. The signal oscillator and chart recorder are electronically or mechanically coupled to ensure synchronisation between the chart drive and the frequency of the acoustic source. Various damping time constants can be applied to the pen movement of the level recorder to minimise noise interference. Normally the frequency sweep has to be performed twice, once for the reference hydrophone and again for the unknown hydrophone. The calibration calculation therefore assumes that nothing changes between the two measurements. A preferred method is to plot the difference signal directly by means of a differential preamplifier and the level recorder.

The calibration accuracy depends on the stability of the acoustic medium, the uniformity of the acoustic field in the test volume and the linearity of the recording instruments. In practice, problems with multipath interference and varying experimental conditions can introduce a variance of ±2 dB or greater in the measurement of the signal level. Post measurement signal analysis can be employed to reduce this level of uncertainty comparable to that of the calibration accuracy of the reference hydrophone.

The swept frequency method has the disadvantage of only measuring the relative RMS signal level between a reference and unknown hydrophone and is rarely used to measure phase and amplitude. In practice the phase can be measured by a connecting a phase meter between the two signals; the relative amplitude response can then be calculated. However, the procedure is laborious and not very accurate. There is an increasing requirement for accurate phase calibration because of techniques used in the signal processing of multi-hydrophone assemblies. This requirement is best met by the FFT method.

2.2 FFT method

The FFT method refers to the spectral analysis techniques employed to determine the relative phase and amplitude relationship between a reference hydrophone and an unknown hydrophone. A specialised instrument is normally used which uses the Fast Fourier Transform technique to compute the relative phase and amplitude. If a dedicated instrument is not obtainable the relevant computations can be performed by a computer and an A/D converter.

The acoustic source is driven by a signal which is no longer a pure sine tone but a combination of frequencies. Usually the signal is not white noise (all possible frequencies excited) but a synthetic spectrum where the discrete frequencies match the discrete analysis frequencies of the instrument. The instrument does not give a continuous frequency analysis of a signal. The time average distribution of the signal frequencies can be made so that all frequencies in the range of interest are equally likely. The power output at any one frequency at any time is therefore low and signal averaging has to be used to improve the signal to noise ratio in the detection process. The effects of multiple reflections within a test tank tend to be smeared out since any pair of signal paths can produce both constructive and destructive interference at any frequency. Similarly the spatial acoustic field, on average, will also be more uniform.

As dedicated instruments are normally used for the signal analysis the methods that are employed in the computations, which are slightly different to normal, are discussed as follows.

The Discrete Fourier Transform (DFT) can be used to describe the frequency content of the sampled time section or series of an unknown signal. The forward transform is:

$$G(k) = \frac{1}{N} \sum_{n=0}^{N-1} g(n) e^{-i2\pi kn/N}$$

where $k = f_k$, $n = t_n$ and N = number of samples.

It can be seen that there is a simple equivalence between the time-function and frequency-function form of a signal. The terminology will be changed to a more convenient form:

$$X(f) = F[x(t)]$$

where the frequency function X(f) is called a linear spectral function or linear spectrum because it corresponds to the first order time function x(t). F is the discrete Fourier transform. The Fast Fourier Transform is actually a computational technique that can rapidly calculate the DFT.

A simple linear system is shown in figure 1. The time function x(t) will be distorted and produce an output y(t). The distortion is known as the impulse response h(t) of the system. Generally the output will also be corrupted by the addition of noise n(t) at the input and m(t) at the output. The Fourier analysis gives a direct equivalence in the frequency domain, that is X(f), H(f), N(f), M(f) and Y(f). In this case H(f) is known as the transfer function, the ratio of amplitude and phase between an input and output.

When X(f) is multiplied by its complex conjugate X*(f) we derive the familiar power spectrum, assuming the independent variable f we can write

$$G_{xx} = X.X^*$$

We can also write the cross power spectrum between two signals as

$$G_{yx} = Y.X^*$$

In contrast to the "auto" power spectrum G_{xx}, the cross power spectrum is usually complex, that is the phase is non-zero. These two power spectrum are central to methods used by the instrument to calculate the transfer function and the coherence function.

It can be shown that, for a perfect system where the noise is absent, the transfer function H can be derived from the ratio G_{AB}/G_{AA} $(=H_1)$ or G_{BB}/G_{BA} $(=H_2)$. Most machines automatically use the ratio of G_{AB}/G_{AA} but can be programmed to use the alternative method. Which technique is preferable is related to the sources of noise in the system.

Consider the generalised system in figure 1, the spectrum analyser actually measures the transfer function between A and B rather than true transfer function H. Thus the power spectrum equations are modified by the presence of noise as follows:

$$A = X + N \quad \text{and} \quad B = Y + M = HX + M$$

Then

$$G_{AA} = G_{XX} + G_{NN}$$

$$G_{BB} = H^2 G_{XX} + G_{MM}$$

$$G_{AB} = HG_{XX} \quad \text{(cross terms are zero)}$$

From these equations we can derive the following relationships for the transfer function H_1 and H_2.

$$H_1 = H/(1 + G_{NN}/G_{XX})$$

$$H_2 = H/(1 + G_{MM}/G_{YY})$$

It can be seen that the H_1 underestimates the true transfer function H due to noise at the input while H_2 overestimates due to noise at the output.

The coherence function measures the correlation between the two signals A and B, if there is perfect correlation there is no noise corrupting the measurement. The formal definition of the coherence function is:

$$\gamma^2 = G_{XX}/G_{XX}\, G_{YY}$$

Using our general model of figure 1 it can be shown that

$$\gamma^2 = \frac{1}{(1 + G_{NN}/G_{XX})(1 + G_{MM}/G_{YY})}$$

That is, the function is proportional to the signal to noise ratios G_{NN}/G_{XX} and G_{MM}/G_{YY}. In the limit of zero noise, or perfect correlation, the coherence function is unity. The measurement of γ^2 gives an indication of the presence of noise but is unable to distinguish between input and output noise. It is possible to calculate(ref.1) the 90% confidence limits on the calculation of the transfer function as a function of the coherence and the number of averages used to obtain the power spectra. These limits are plotted in figure 2.

The preceding discussion has only referred to the measurement of a single input "one stage" system, for example a preamplifier used in the calibration process. The hydrophone calibration is made by comparing the relative output between a reference and unknown hydrophone. The procedure includes a number of stages including the recording and replay of tapes. In this case the system shown in figure 3 applies. Each arm of the measurement chain involves a number of transfer functions and noise sources. The spectrum analyser measures the transfer function between A and B, what is required is the ratio of the transfer functions H_{IR} and H_{IU}

where H_{IR} and H_{IU} are the transfer functions of the reference and unknown hydrophones when converting the sound pressure wave S to an electrical signal.

$$H_A = H_{1R} \cdot H_{2R} \cdot H_{3R} \cdot H_{4R}$$

Consider the reference chain in figure 3(a) the output at A is given by

$$A = ((((S + N_{AR})H_{1R} + N_{1R})H_{2R} + N_{2R})H_{3R} + N_{3R})H_{4R} + N_{4R}$$

The set of transfer functions can be replaced by a single transfer function.

Let

$$H_A = H_{1R} \cdot H_{2R} \cdot H_{3R} \cdot H_{4R}$$

The non acoustic noise can be replaced by a new function M_A where

$$M_A = N_{1R} H_{2R} H_{3R} H_{4R} + N_{2R} H_{3R} H_{4R}$$

$$+ N_{3R} H_{4R} + N_{4R}$$

If

$$N_A = N_{AR} \qquad \text{(acoustic interference)}$$

Then

$$A = (S + N_A)H_A + M_A$$

We may simplify in a similar manner for the "unknown hydrophone" channel. The system now simplifies to that shown in figure 3(b) and using the same approach as described for a simple system we have for the reference channel

$$X_A = S + N_A$$

$$A = Y_A + M_A = H_A(S + N_A) + M_A$$

Thus

$$G_{AA} = H_A^2 (G_{SS} + G_{NNA}) + G_{MMA}$$

Similarly

$$G_{BB} = H_B^2 (G_{SS} + G_{NNB}) + G_{MMB}$$

and

$$G_{AB} = H_A H_B G_{SS} \qquad \text{(cross terms zero)}$$

If the transfer function TF between A and B is measured using G_{AB}/G_{AA} we have:

$$TF = \frac{H_A H_B G_{SS}}{H_A^2 (G_{SS} + G_{NNA}) + G_{MMA}}$$

$$= \frac{H_B}{H_A} \cdot \frac{1}{1 + \frac{G_{NNA}}{G_{SS}} + \frac{G_{MMA}}{H_A^2 G_{SS}}}$$

As may be intuitively expected the transfer function is proportional to the ratio of all of the transfer functions in the recording chain and is sensitive to the magnitude of the noise sources. The term $G_{MMA}/H_A^2 G_{SS}$ is a term that represents all of the electrical noise inputs modified by a series of transfer functions. In practice the acoustic noise G_{NNA} is the predominant noise source and the measurement accuracy becomes proportional to the signal to noise ratio as previously described, figure 2 applies again. The coherence function $G_{AB}^2/G_{AA} G_{BB}$ is given by

$$\gamma^2 = \frac{H_A^2 H_B^2 G_{SS}^2}{[H_A^2(G_{SS} + G_{NNA}) + G_{MMA}] [H_B^2(G_{SS} + G_{NNB}) + G_{MMB}]}$$

If we assume the dominant noise source is acoustic and is identical for both hydrophones, we may write $G_{NNA} = G_{NNB} = G_{NN}$. Then the coherence function simplifies to

$$\gamma^2 = \frac{1}{1 + \frac{G_{NN}^2}{H_A^2 H_B^2 G_{SS}^2}}$$

that is, proportional to the signal to noise ratio. In summary, the pressure sensitivity of an unknown hydrophone is found by measuring the transfer function between its amplification chain and a reference hydrophone's chain when both are subject to the same acoustic field. All elements in the amplification chain are measured to find their absolute or relative transfer functions and the inverse of these values are used to multiply the original transfer function such that the ratio of the reference hydrophone and unknown hydrophone transfer functions remains.

The measurements produced by the FFT analyser are at discrete frequencies by the definition of the Discrete Fourier Transform. The discrete frequencies are produced by a digital filtering process which, if ideal, would have a rectangular shape centred at each frequency and a width equal to the frequency spacing. The filter spacing is equal to the inverse of the sampe time. In reality the filter has a passband shape which results in "cross-talk" between adjacent bins and amplitude and frequency resolution uncertainty. Various filter shapes can be created which represent a compromise between these factors. Consider figure 4, as shown, the filter to filter spacing Δf is fixed by the sampling rate. As the actual spectral line moves from $N\Delta f$ to $(N+1)\Delta f$ it traces out the passbands as shown. The maximum uncertainty is when a component falls midway between the filters, as a passband becomes flatter on top the uncertainty is reduced - but so is the frequency resolution.

The "flat top" passband is optimised for minimum amplitude uncertainty but has poor frequency resolution. It is normally used for measuring discrete spectral lines. The "Hanning" passband is a common compromise between the "flat top" and "uniform" and is usually used for random noise measurements. This is the window function selected for the tape replay analysis of the primary acoustic records. When real time analysis is performed the "uniform" passband and the analyser's built-in Periodic noise source is used.

An analyser noise source may be one of several types, also, some manufacturers use a different nomenclature to describe the type. The following nomenclature applies to the HP series of analysers. Normally there are two different types: Random and Periodic. Random is a signal sequence where the phase and amplitude are unrelated and not repeated. It is therefore an approximation to white noise, after some time all frequencies are generated with an equal amplitude distribution and random phase relationship. Measurements may take a long time but true white noise excitation is assured. The Hanning window function is normally used with this source.

The Periodic noise is a pseudo-random frequency sequence of length T which is repeated after each period of time T. It is periodic and therefore has energy only at discrete frequencies. The period length T is matched to the record length of the analyser, so the frequency components of the pseudo-random signal coincide with the computed lines in the analyser. Thus the Uniform filter, which has the best frequency resolution, will improve the signal/noise ratio of the measurement as it will reject those frequencies not attributable to the noise source.

Some machines use a pseudo random generator sequence to generate the Random noise source. In this case the sequence length T is so long (up to 14 min) that in many cases it is much longer than the analyser's integration time. The Random noise source of the H3582A analyser was used as its "Perodic" spectrum would not have matched the analyser frequency bins of the HP5420A used at the laboratory.

3. EXPERIMENTAL DETAILS

3.1 General details

The facility at the South Para reservoir consists of a raft about 30 m from the shore and an on-shore instrumentation van. Two multicore screened cables connect the van to the raft. The projector, which is suspended 12 m below the raft, is remotely powered from the van. The hydrophone signals are amplified on the raft by battery powered amplifiers before transmission to the van and, if required, can be recorded on a portable tape recorder on the raft. The equipment required for swept frequency calibration is rather bulky and can only be operated at the van where mains power is safely available. In the case of FFT analysis, tape recordings are made of the signals on board the raft, in this manner the problems of hum and noise pickup in the 50 m signal cable to the van are removed. As a backup, monitoring and some analysis is done at the van with a portable FFT analyser.

The acoustic source used was a J-9 projector with a nominal frequency range of 40 Hz to 5 kHz. The projector was driven by a 30 W amplifier and operated near the maximum power output. The signal source depended upon the calibration method being used. The array module and the M115C reference hydrophone were suspended approximately one metre from the radiating face of the J-9 on the acoustic centre line. When the swept frequency method was used the reference hydrophone was suspended about 150 cm from the array otherwise it was taped onto the appropriate part of the array. The whole system was operated at about 12 m depth so that the dominant acoustic reflecting surfaces were equidistant.

Weather conditions during the two days of experiments were fine with light and variable 10 kn wind. The resultant slight movement of the raft had some effect on the swept frequency method as noted in the following description of the experimental details.

3.2 Swept frequency

A swept sine wave oscillator, B&K type 2010, was the signal source for the J-9 projector. Using a B&K level recorder type 2307 the signal from either the reference or the array hydrophones was recorded on an annotated frequency vs power chart. The chart recorder and oscillator were mechanically coupled to syncronise the chart movement with the frequency sweep. The signal gains were adjusted on the raft to ensure similar levels at the chart recorder. The oscillator was swept at a logarithmic rate over the range 30 Hz to 3 kHz taking about 10 s. Three sets of traces were overlaid so that the mean of the peaks and troughs in the traces could be estimated by eye. Small scale harmonically related oscillations were observed and are due to multipath effects, any variation in the mean value is due to the movement between the signal source and the hydrophone under test. For example, a 100 mm movement at 1 m separation between the projector and hydrophone will result in approximately 2 dB signal change.

The difference between the reference and the test signal was measured on a point to point basis from the smoothed curves. Taking into account the known gain/slope characteristics of all amplifiers and the quoted sensitivity of the reference hydrophone, the sensitivity of the array section under test could then be calculated at discrete frequencies.

It is possible to apply a smoothing algorithm to the data to remove the harmonically related oscillations that may be apparent in the recordings. This process is fully described in Appendix I. Tests were only performed on array AM13, all results are presented in Table 1.

3.3 FFT

The Random noise generator from the 3582A spectrum analyser was used set to a bandwidth of 2.5 kHz and used as the signal source for the J-9 projector. The portable analyser was also used for on-site analysis, the coherence function analysis mode was used to check the "validity" of the received signals and to check the transfer function between the two signals.

The reference hydrophone and a hydrophone group of AM 13 were suspended 150 mm apart and 1 m from the projector. The projector was operated at 30 W output power using the random noise generator as the signal source. The coherence function was measured with the HP 3582A at the van using 128 signal averages. A very high coherence was noted from 40 Hz to 2.5 kHz, with slight dips at 50 Hz and 100 Hz. The experiment was repeated with the reference hydrophone taped onto the array to help location and handling problems. It was thought that mechanical noise may couple between the reference hydrophone and the array, however, the coherence measurement was identical to the freely suspended case indicating that any measurements of the transfer function would be valid. Therefore for experimental convenience the reference hydrophone was taped on.

The same procedure was adopted for the other MSC experimental arrays AM 10, 11, 12 and AUSTAM. The hydrophone was taped on to the hydrophone section under test and the array was lowered to the correct depth. The gains were adjusted on the raft to give approximately -10 dB signal into the tape recorder on the raft. The signal "quality" was checked at the van by means of the HP 3582A coherence function. A short time (10 s) was usually required for the array to stop oscillating after it was deployed but, after settling, extremely high coherence was observed for all hydrophone assemblies in the range 40 Hz to 2.5 kHz. The hydrophone signals were recorded at the raft for 3 min on a TEAC R-81 tape recorder operating at 7½ ip/s using TDK AD120 tape. Simultaneous spectral analysis was performed by the HP 3582A at the van. Plots were made of the transfer function amplitude and phase and also the coherence function. The analyser is only able to give linear frequency plots nevertheless they acted as a primary record backup. The tape recordings of the signals obtained on the raft were used for the more complete analysis using the HP 5420A in the laboratory.

The HP 5420A performs spectral analysis over 256 frequency bins when used in the transfer function mode. The machine can measure the transfer function between two signals and the coherence function via measurement of the auto and cross power spectra. The machine has the capability to multiply spectral plots by other stored plots. In this way a preamplifier transfer function can be removed from a measured signal response to derive the true transfer function. Similarly, as the response of the reference hydrophone is known the sensitivity curve for the array can be derived by multiplication of the transfer function with the calibration curve of the reference hydrophone. The latter curve is supplied by the manufacturer and is usually entered as a linear function between certain frequency limits.

3.4 The analysis and recording chain

In deriving the final sensitivity curve via the transfer function the response of the whole recording and playback chain must be considered. The preamplifier transfer function was measured over the recording frequency by the injection of random noise in the previously described manner. The result was stored in the HP 5420A to enable calculation of the sensitivity curves. The tape recording system was nominally set up to be transparent, that is, a through gain of unity for each channel. However, the responses of the tape recorders was checked as follows:

3.4.1 Determination of optimum recording level

TDK AD120 tape was used at $7\frac{1}{2}$ ip/s in the TEAC R-81 recorder. Random noise was input to either channel 1 or 2 and the transfer function between input and output was measured by the HP 5420A. The input signal level was varied between - 20 dB to + 4 dB as measured by the tape recorder meter. The transfer function amplitude and coherence was then measured using up to 128 averages over the frequency range 0 to 1.2 kHz using a Hanning window function. Phase is not measured as the finite gap between the record and reply head will introduce a linear phase shift.

3.4.2 Determination of transfer function before and after playback

The calibration technique depends on the measurement of the transfer function between two channels. The normal assumption is that any component, for example, tape recorder or coaxial cable, that is common to the two channels will have identical signal transfer characteristics. This test was designed to check the relative recorded signals between channels. Random noise was recorded at $7\frac{1}{2}$ ip/s on tracks 1 and 2 of the raft tape recorder using TDK AD120 tape, - 20 dB recording level and 1.2 kHz bandwidth. The recording level was the same as that used in the experiments. The tape was then played back on the analysis tape replay machine which is a similar TEAC. The transfer function between channels 1 and 2 were then measured by the HP 5420A in the normal way.

4. CALIBRATION RESULTS

4.1 Swept frequency - hand processed

The swept frequency chart records are difficult to reproduce in this report. The curves were digitised and processed by a computer and a typical result is shown in figure 5. The absolute levels are not shown in this figure as it only serves to show the typical shape of the curves. The sensitivity of array AM13 at spot frequencies was derived by the technique described in Section 2.2 and the resultant plot is shown in figure 6. The calculations assumed a linear preamp response in the frequency range of interest with a gain of 54 dB at 100 Hz and a gain slope of 6 dB/octave. The calculated sensitivity for each hydrophone element is listed in Table 1.

4.2 Swept frequency - computer processed

Using the techniques described in Appendix I, the difference signal was generated and is shown in figure 7. This signal was then multiplied by a constant slope function which was equal to the low frequency, 50 to 200 Hz, gain response of the preamplifier as used in the hand processed calculations. The Fourier spectrum of the difference signal and that of a suitable smoothing window is shown in figure 8. The result of applying the window is seen in figure 9 which is the difference signal without multiplying by the preamp gain. No serious attempt has been made to quantify these results other than to demonstrate that a reduction in the signal variance is obtained. Calculation from the smoothed curve with the known preamp response gives agreement with the random noise technique to ±1 dB over the frequency range 50 Hz to 1 kHz.

4.3 FFT analysis

The tape recordings of the acoustic records were analysed using the HP 5420A spectrum analyser. The transfer function between the reference and

unknown hydrophone was divided by a pseudo generated array preamp transfer function. The function had a fixed slope and a set gain at 100 Hz obtained from prior spot frequency measurements of the array preamp. The resultant function was then divided by the transfer function of the raft preamp, and knowning the voltage sensitivity of the reference hydrophone at a spot frequency, the voltage sensitivity spectrum of the unknown was plotted.

The resultant plots for all of the arrays are shown in figures 10 to 13. The sensitivity figure shown in the plots, and summarised in Table 1 is at a frequency of 100 Hz. The sensitivity outside this frequency is influenced by the deviation of the assumed slope preamp from the actual slope. Measurements conducted by other means indicate that the actual gain at any frequency was within ±¼ dB of that calculated from the slope.

4.4 Tape recorder characteristics

The measurements of the optimum recording level are shown in figure 14. The results indicate that minimal 50 Hz and harmonic inteference is reached at the -10 to 0 dB recording level, not -20 to -10 dB as has been used before.

5. SOURCES OF ERRORS

The measurement of the transfer function between a reference hydrophone and the unknown hydrophone requires accurate measurement of the transfer function in all parts of the measurement chain for each transducer. Alternatively, where the recording chain components are the same for both measurement channels a common test signal may be injected and the relative, channel to channel, transfer function can be measured. In this FFT calibration procedure the interest is in relative levels hence any common gain and phase shift will not affect the measurement. This is the reason why AM tape recording may be used even though the frequency response may not be ideal.

However, the record and replay settings may be the same for one machine but different on the replay machine. More important, any relative tape head misalignment between machines will affect the relative phase and hence the magnitude of the replay of a signal simultaneously recorded on another machine. The following transfer functions were measured, either as an input/output ratio or as a channel/channel ratio.

(a) Raft amplifiers which drive the tape recorder channels 1 and 2.

(b) Record/replay on channels 1 and 2 of both tape recorders, measured for future reference.

(c) Between channels 1 and 2, and 1 and 7 of the analysis laboratory tape recorder when a sample tape had pre-recorded noise recorded by the raft tape recorder.

These transfer functions are shown in figures 15, 16, 17, 18 respectively. In particular, note that there is a phase shift between channels when method (c) is used. However, it was found that the magnitude of the transfer function was unity from 10 Hz to 1 kHz for channels 1 and 2 and would therefore not affect the FFT measurement. Figure 18 shows that there is a slight tape head misalignment between channels 1 and 7 and should be taken into consideration if these channels were used.

As mentioned earlier the accuracy of the measurement of a transfer function is also dependent on the coherence of the measurement. Assuming 256 measurements and a coherence of 0.9 (see figure 2) an error bound of ±0.2 dB may be placed

on the transfer function measurement. Other error bounds are derived from experimental observations or stated tolerances and are listed below:

Calibration accuracy of ref hydrophone	±0.5 dB
Preamp gain at 100 Hz	±0.1 dB
Preamp gain at other frequencies	±0.25 dB
A/D limitations	±0.01 dB
Measured transfer function (coherence .9)	±0.2 dB
Gain match in tape recorders	±0.2 dB

The overall accuracy of the derivation of the hydrophone sensitivity is the square root of the sum of the square of the errors in linear units which amounts to ±0.6 dB. For most measurements the errors are dominated by the reference hydrophone accuracy. The sensitivity of the hydrophone assemblies is listed in Table 1 with 90% error bounds derived from the above list of error bounds.

6. CONCLUSIONS AND RECOMMENDED CALIBRATION PROCEDURE

In conclusion it can be seen that the FFT method gives a rapid "easy to visualise" measurement procedure. Error sources can be measured and the validity of the measurement can be checked at any frequency by means of the coherence function. By comparison, the swept sine method is greatly influenced by the measurement conditions and the induced errors are not readily removed.

Based on the practical experience obtained in the calibration of the array hydrophones using the random noise technique the following may be used as a recommended procedure for similar calibration runs at the South Para facility.

- The reference hydrophone shall be taped to the acoustic centre of the hydrophone assembly.
- The assembly shall be at half of the available water depth.
- The assembly shall be on the acoustic centre line of the projector.
- Due regard shall be taken of the assembly length, its distance from the projector and the upper frequency limit because of field curvature and near-field effects. As an approximation with 1 kHz upper limit and 800 mm assembly the separation should be greater than 400 mm. Thus for most practical systems 1 m is a reasonable compromise between this effect and signal/noise criteria.
- Tape recordings shall be made at the raft of the output from the hydrophones. Suitable amplification should be made to record at 0 dB, 7½ ip/s tape speed. Three minute recordings shall be made for each run. The recording time specified is for a 1.6 kHz analysis bandwidth, using the HP 5420A analyser and 256 averages. The time required is approximately inversely proportional to the bandwidth and can be calculated from T(min) = 4.5/BW(kHz).
- A recording shall be made of the ambient noise before and after the entire calibration run.
- All amplifier gains and any other conditions must be noted.

- The J-9 shall be driven from the built-in random noise generator of the HP 3582A spectrum analyser. This analyser shall also monitor the hydrophone outputs and shall be set-up as follows:

- Measure transfer function and coherence.

- 128 averages.

- Hanning window function.

- Select required bandwidth.

- The amplitude and phase should be well behaved and the coherence should be approximately unity beyond 50 Hz. Any deviation from this shall be investigated - possible problems could be: low acoustic signal, mechanical coupled noise between the reference and unknown hydrophone, interfering noise source, bad electrical connections.

- The noise source shall be coupled directly to the channels being used on the tape recorder and a 3 min recording made. This is to check tape head alignment.

- All tape records are to be analysed at the laboratory using a suitable spectrum analyser.

REFERENCES

No.	Author	Title
1	Bendat, J.S. and Piersal, A.G.	"Random Data: Analysis and Measurement Procedures". Wiley 1971
2	Bobber, R.J.	"Inteference Versus Frequency in Measurements in a Shallow Lake". J. Acoust. Soc. Am. 33, 1211-1215, 1961

APPENDIX I

SMOOTHING OF CALIBRATION TRACES OBTAINED IN HYDROPHONE CALIBRATION

When an underwater transducer calibration is made there is invariably multipath acoustic reflections from nearby objects and the surface. These reflections give rise to constructive and destructive interference of the received acoustic signal as a function of frequency. Normally a subjective assessment is made of the received signal vs frequency plot to obtain an average "smoothed" plot. The dimensions of the test site at the South Para Reservoir are such that the magnitude of the variation of the average signal are in practice quite small, ±2 dB being typical. The interference pattern can be approximated as a harmonic series(ref.2) however, a random variation in signal strength is also superimposed due to the relative drifting between components.

The common method to smooth such signals is to apply a running mean. This operation is equivalent in Fourier terms to the convolution in the function domain of the signal function with a rectangular function of width W and unit amplitude. The same result is obtained by multiplication in the frequency domain of the frequency transform of the time domain signal and window function and then taking the inverse transform to reconstitute the smoothed signal. The advantage of working in the frequency domain is that the harmonic content of the signal can be readily identified and the window width adjusted to optimise the rejection of these components.

An interactive computer program was written which would perform the smoothing process described above on supplied data. The data was produced by digitising the signal vs frequency plots obtained from the B & K signal analyser. One set of data was of the reference hydrophone, the other set was of the test hydrophone. The program performs a splining operation and there is then an option to operate on either plot or the difference between them. The Fourier transform of the sample is displayed and is normalised to the largest amplitude frequency component. The window width is selected and its transform is overlaid. By varying the window width an optimum value may be obtained where the nulls of the window spectrum coincide with the peaks of the sample spectrum. The multiplication is then performed in the frequency domain, and by means of the inverse transform, the smoothed sample is obtained.

Examples of the interactive procedure are given in figures 19 to 23. Figure 19 shows two typical plots obtained after digitising the output from the B & K level detector, one is the reference hydrophone signal, the other is the test signal. The difference signal is shown in figure 20 while in figure 21, which has a linear frequency scale, the periodic nature of the interference can be more readily seen. This can also be seen in figure 22 which is an indication of the spectral content of the difference signal. The DC component is suppressed and the graph is normalised to the next frequency component. Overlaid is the transform of a unit amplitude window of width 111 bins. The resultant transform of the multiplied signal is seen in figure 23. A further development of the computer program will enable this signal to be multiplied by any other gain function so that a direct plot may be made of the sensitivity of the test hydrophone. However, this example demonstrates the power of the technique and its more justifiable method of smoothing rather than an operator's interpretation.

TABLE 1. SENSITIVITY OF ARRAY HYDROPHONE GROUPS

Array	Hydrophone Group	Sensitivity dB re 1 V/µPa at 100 Hz
AM11	1	- 210.7 ±0.6
	2	- 210.7 ±0.6
	3	- 209.5 ±0.6
AM12	1	- 208.0 ±0.6
	2	- 207.9 ±0.6
	3	- 208.1 ±0.6
AM13	1	- 219.4 ±0.6
	2	- 206.9 ±0.6
	3	- 212.9 ±0.6
	4	- 208.1 ±0.6
AUSTAM	1	~- 270 (Capacitor)
	2	- 207.9 ±0.6
	3	- 208.6 ±0.6
	4	- 210.7 ±0.6
	5	- 212.8 ±0.6
	6	- 207.3 ±0.6
	7	- 217.5 ±0.6

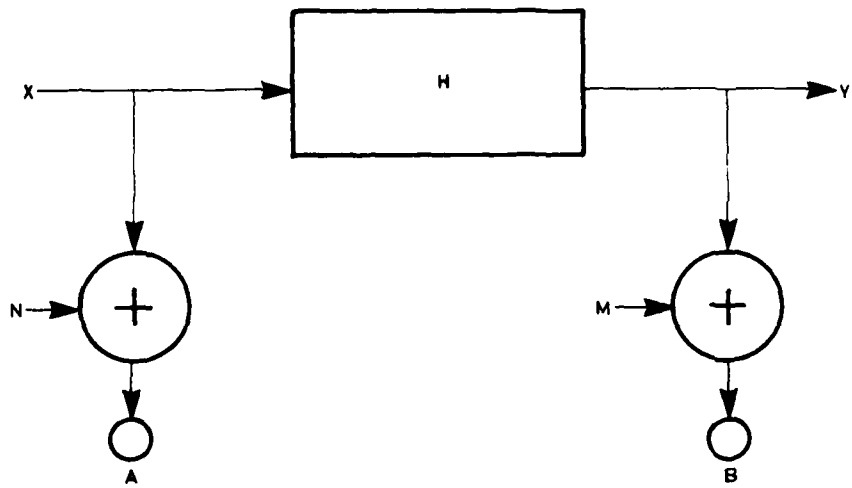

Figure 1. An ideal linear system. The input spectrum X is transformed by H to the output spectrum Y. Noise, N and M, is present and added to the spectra when the transfer function is measured between A and B

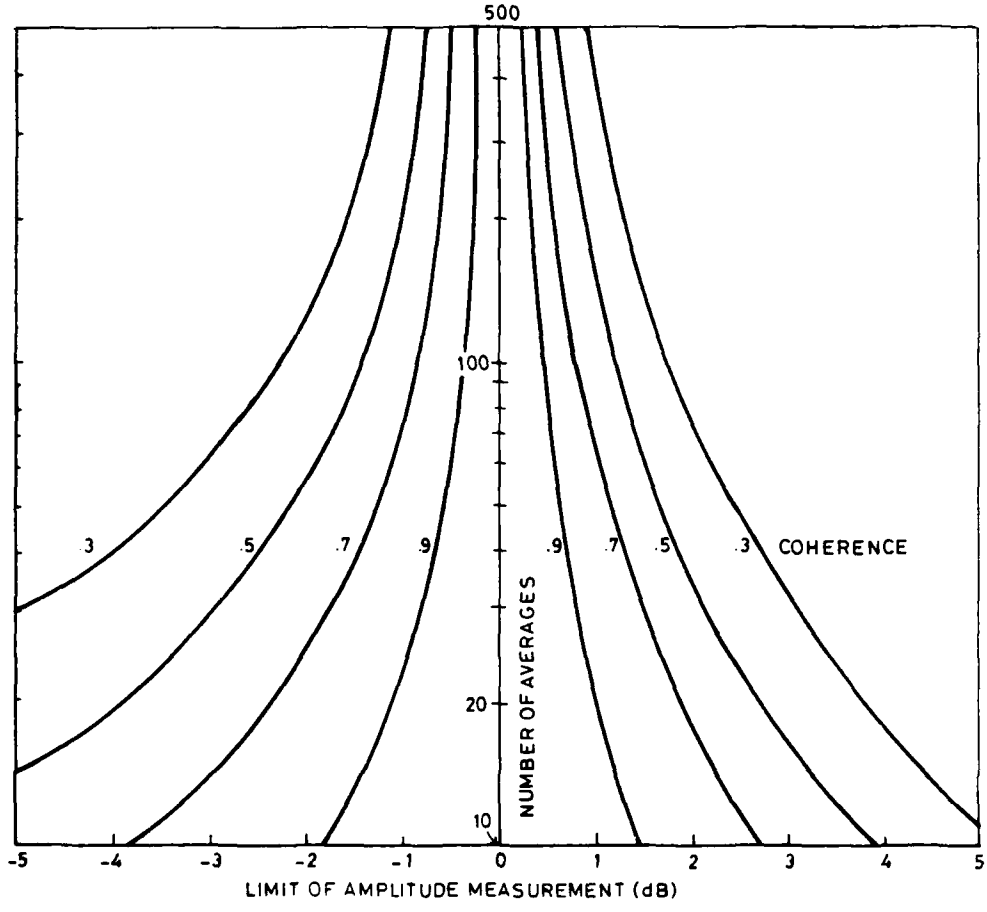

Figure 2. A plot of the 90% confidence limit on an amplitude measurement as a function of the number of averages for various values of coherence

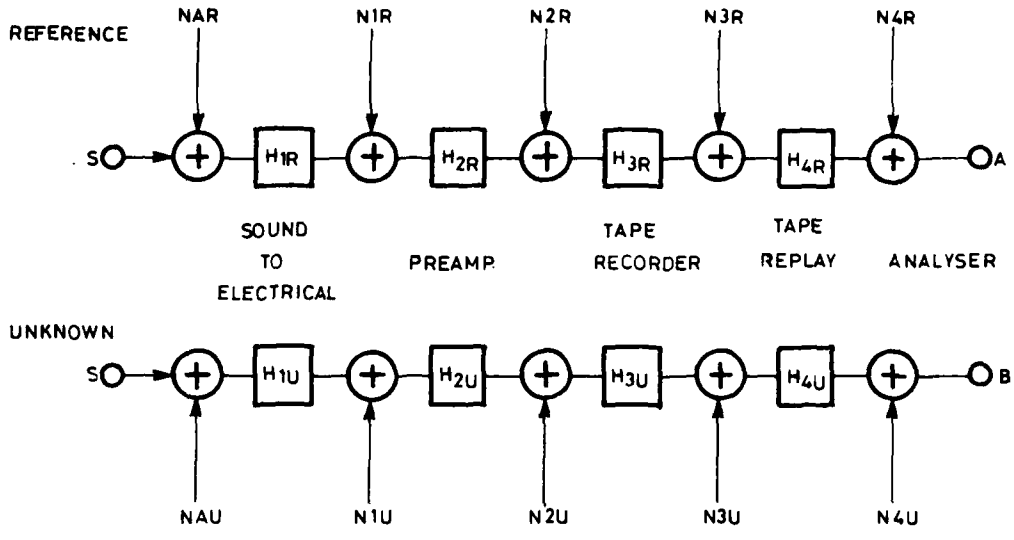

Figure 3(a). The reference and unknown hydrophone measurement system. The analyser measures the transfer function between A and B

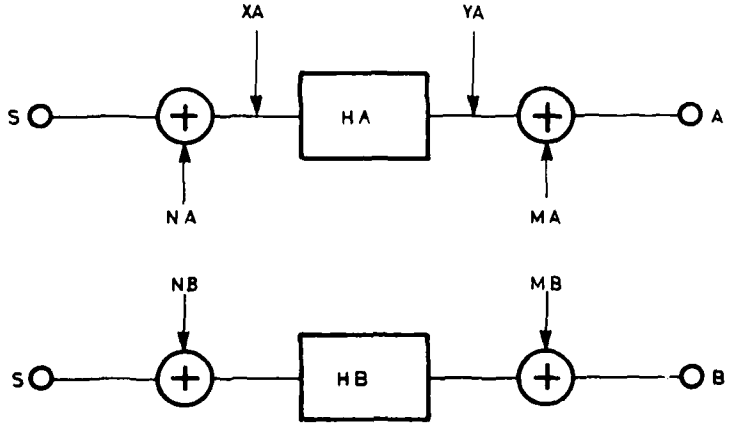

Figure 3(b). A simplified version of (a)

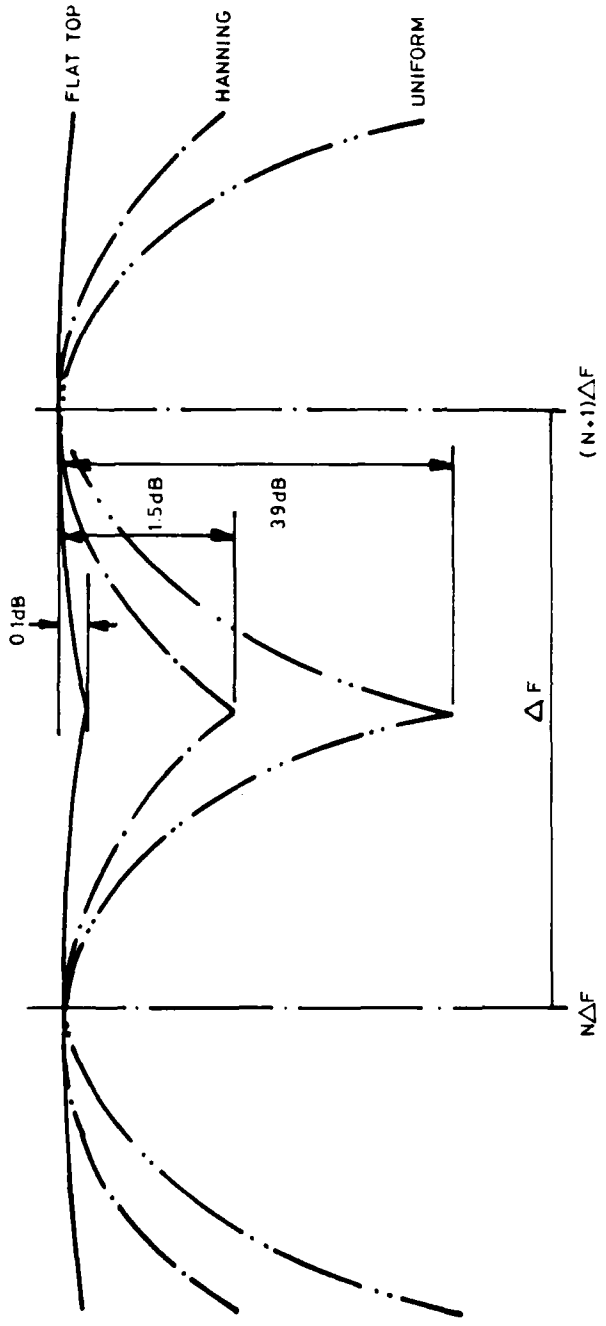

Figure 4. The filter passband shapes for Flat Top, Hanning and Uniform functions. Δf is the filter spacing between the Nth and (N+1)th filter frequency

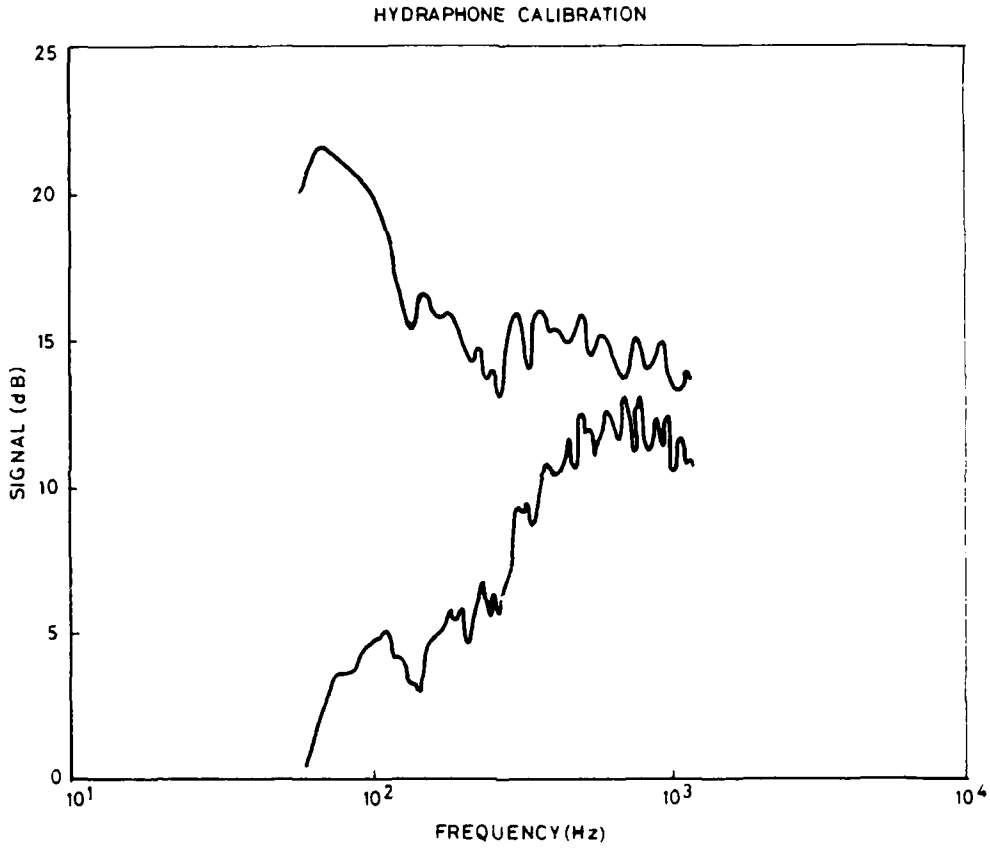

Figure 5. A typical digitised swept frequency calibration plot. The upper curve is the reference hydrophone output and the lower is the array output. The vertical scale represents a relative response

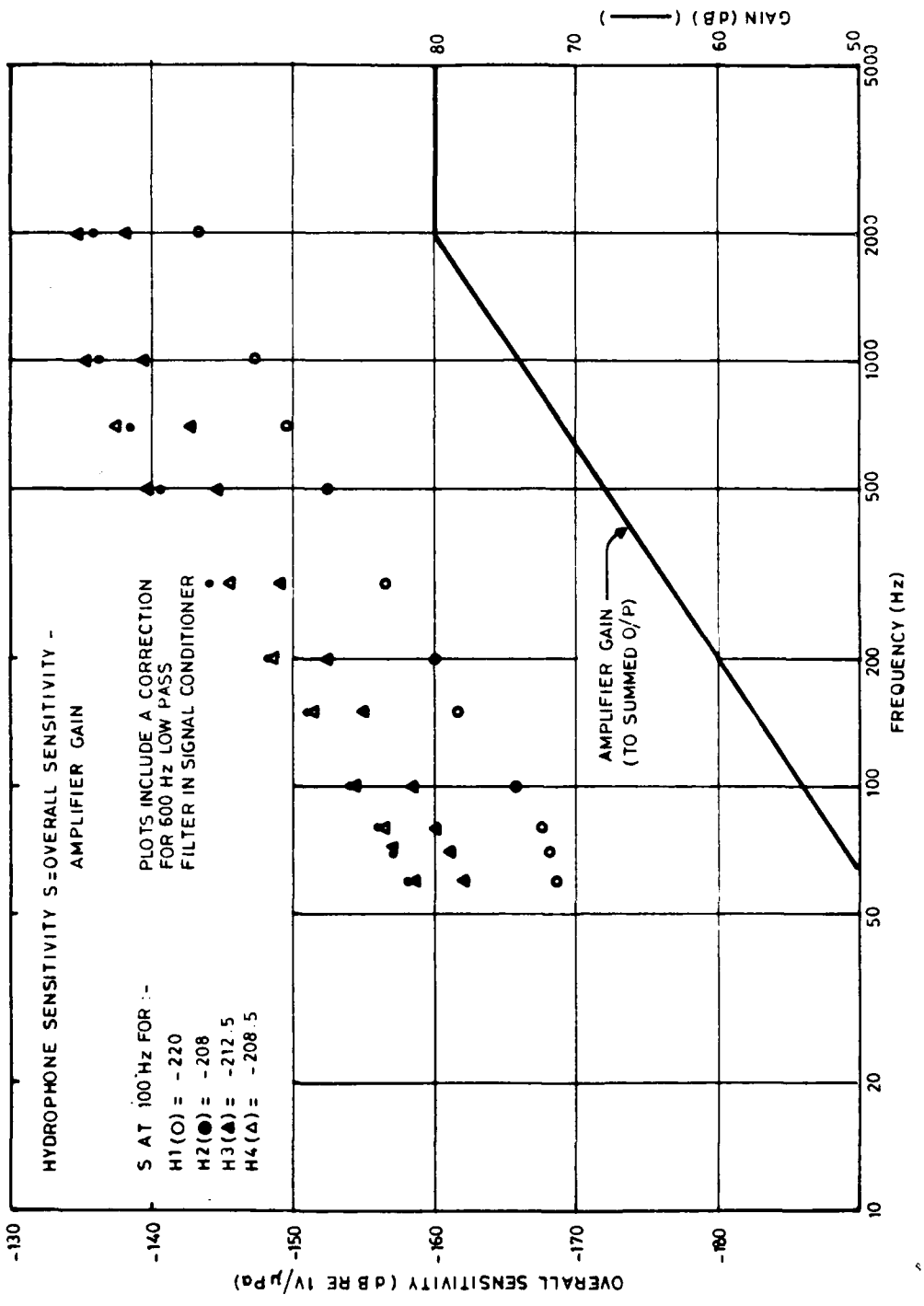

Figure 6. A plot of the overall sensitivity and amplifier gain for array AM13. The hydrophone sensitivity S is equal to overall sensitivity minus amplifier gain and is tabulated for 100 Hz

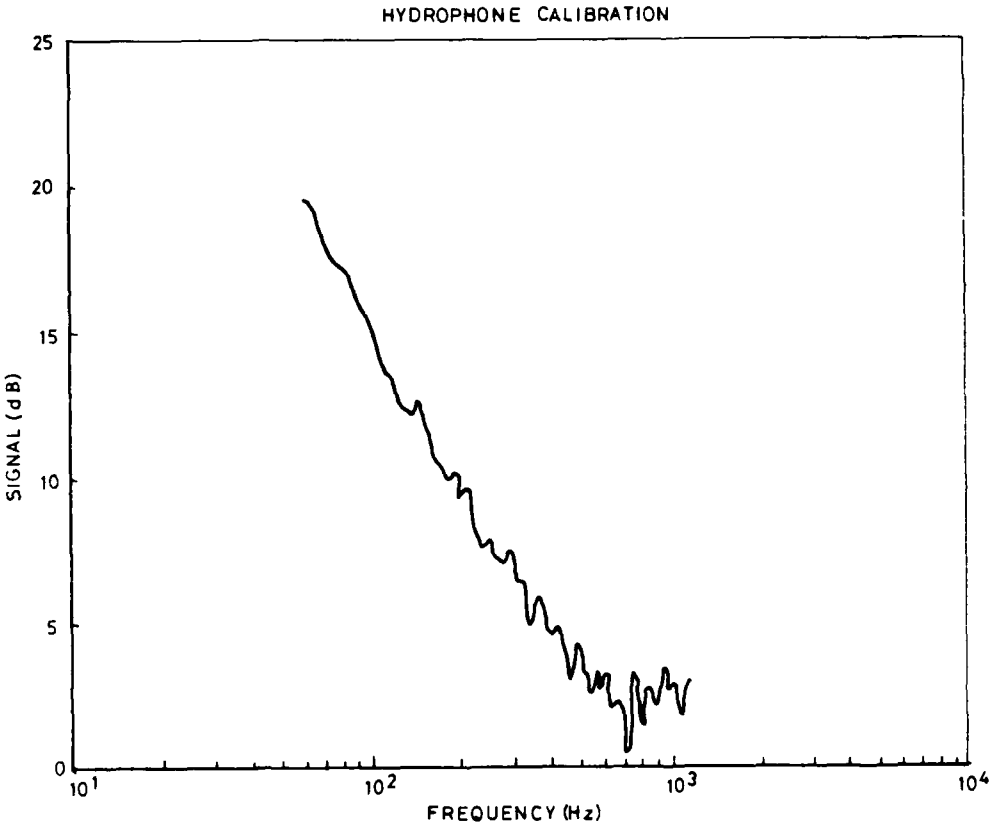

Figure 7. A plot of the sensitivity difference between the reference and an unknown hydrophone. The plot is derived from the two response curves plotted in figure 3

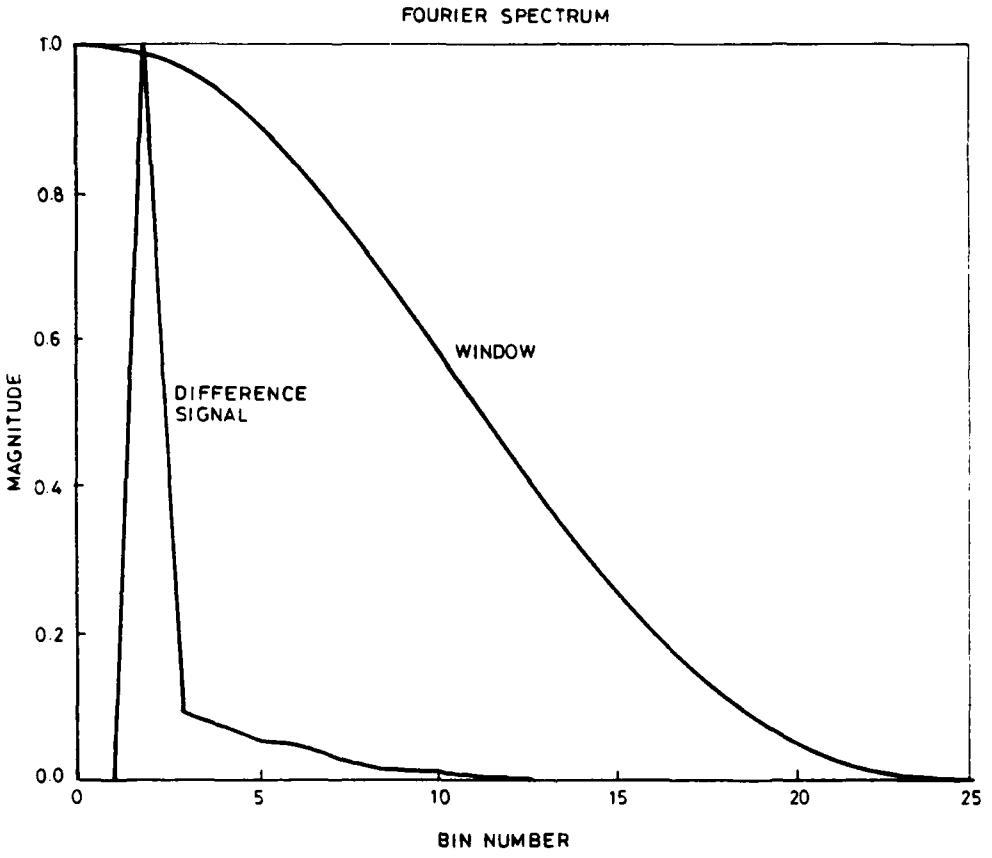

Figure 8. A plot of the first 25 frequency bins of the normalised Fourier spectrum of the difference curve of figure 5 and a window of width 44 bins

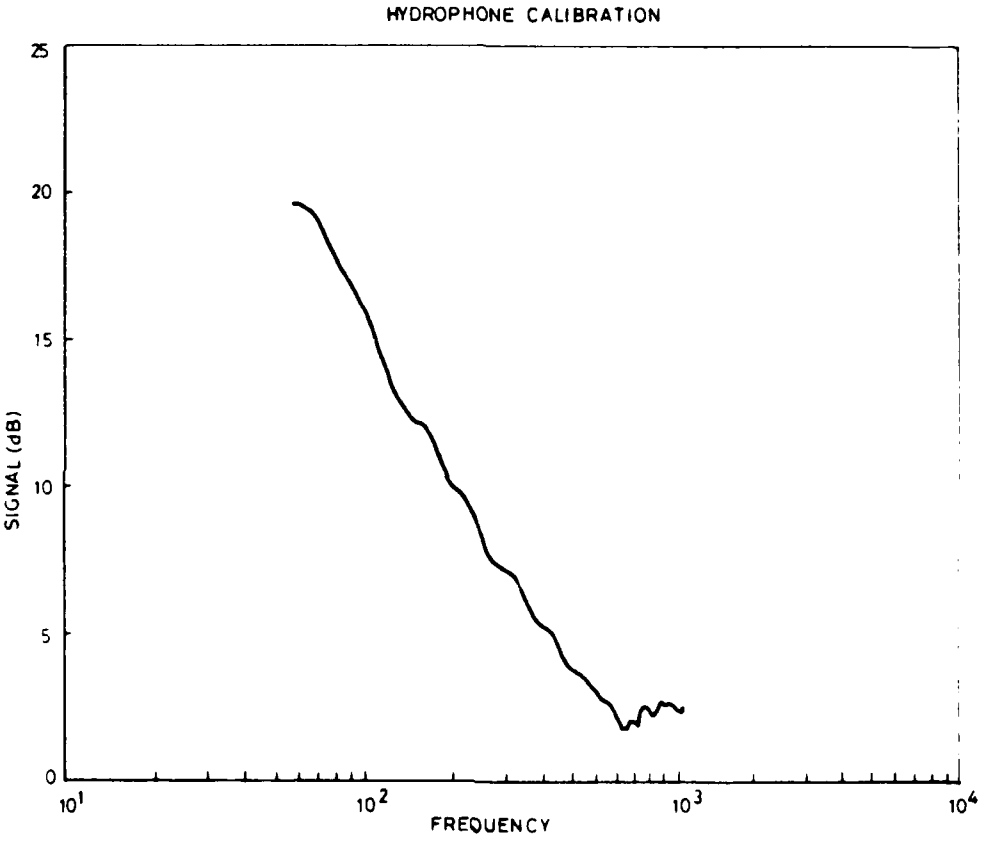

Figure 9. The smoothed difference curve resulting from the multiplication in frequency space of the original difference curve and window spectra and applying the inverse Fourier transform

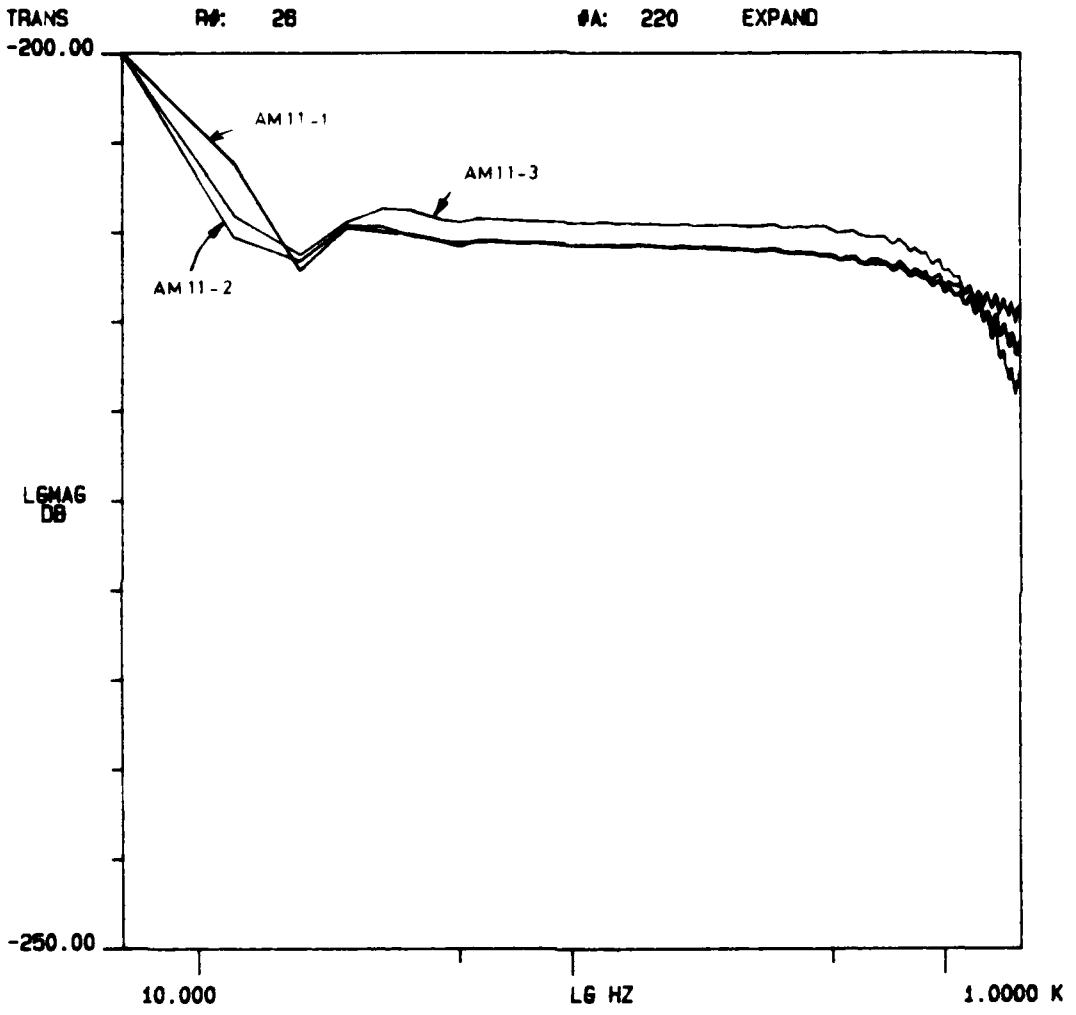

Figure 10. A plot of the sensitivity in dB re 1 V/μPa versus frequency for array AM12. Each hydrophone group is indicated

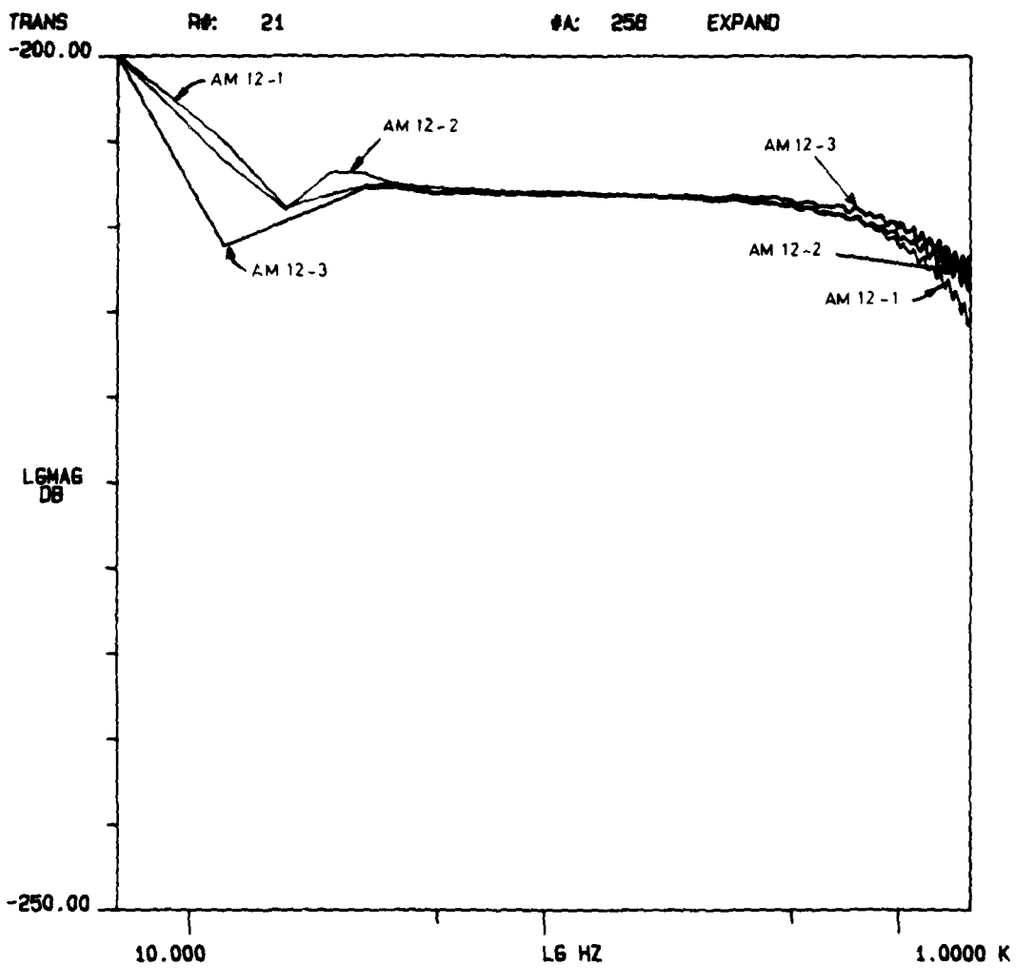

Figure 11. A plot of the sensitivity in dB re 1 V/μPa versus frequency for array AM12. Each hydrophone group is indicated

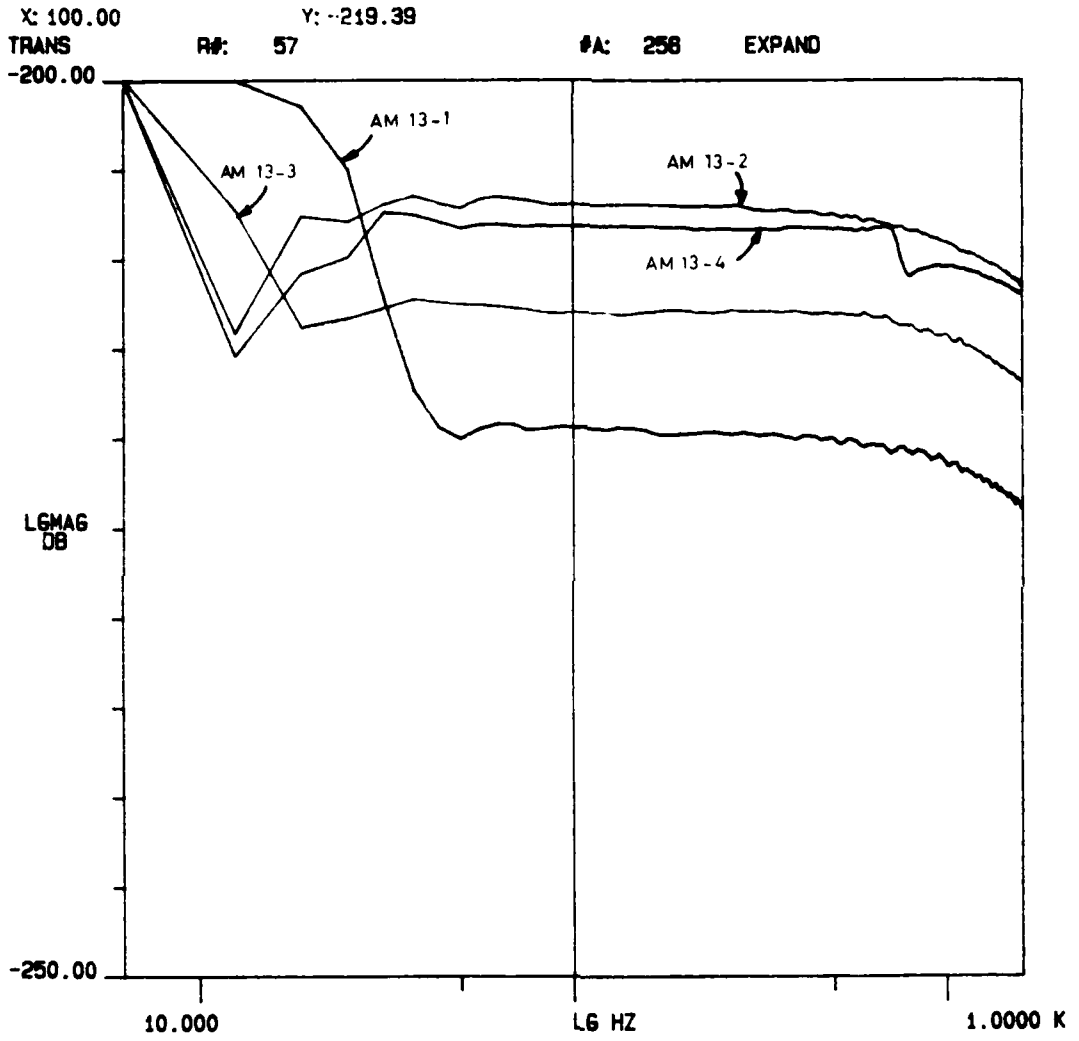

Figure 12. A plot of the sensitivity in dB re 1 V/μPa versus frequency for array AM13. Each hydrophone group is indicated

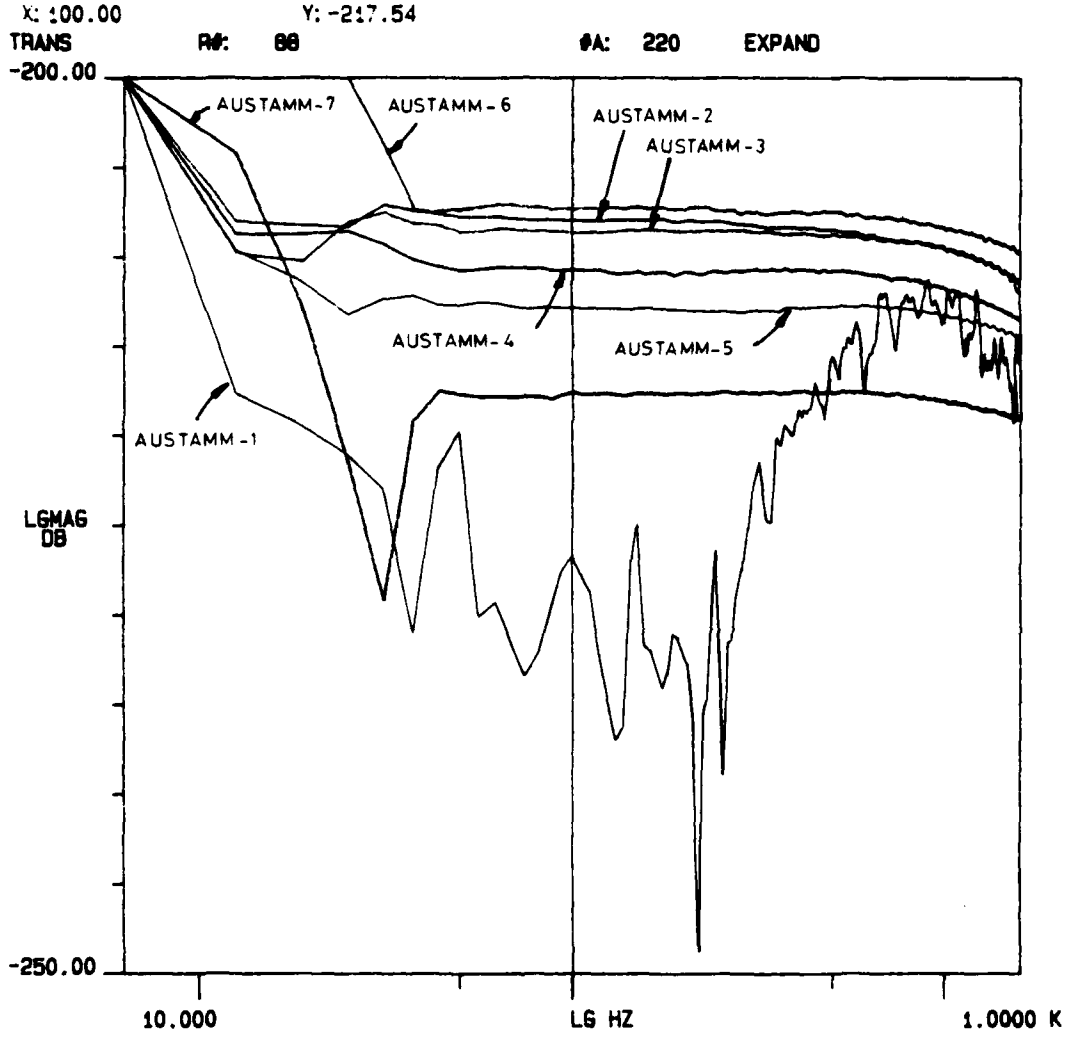

Figure 13. A plot of the sensitivity in dB re 1 V/μPa versus frequency for array AUSTAM. Each hydrophone group is indicated. The curve for the capacitor should be decreased by a further 40 dB

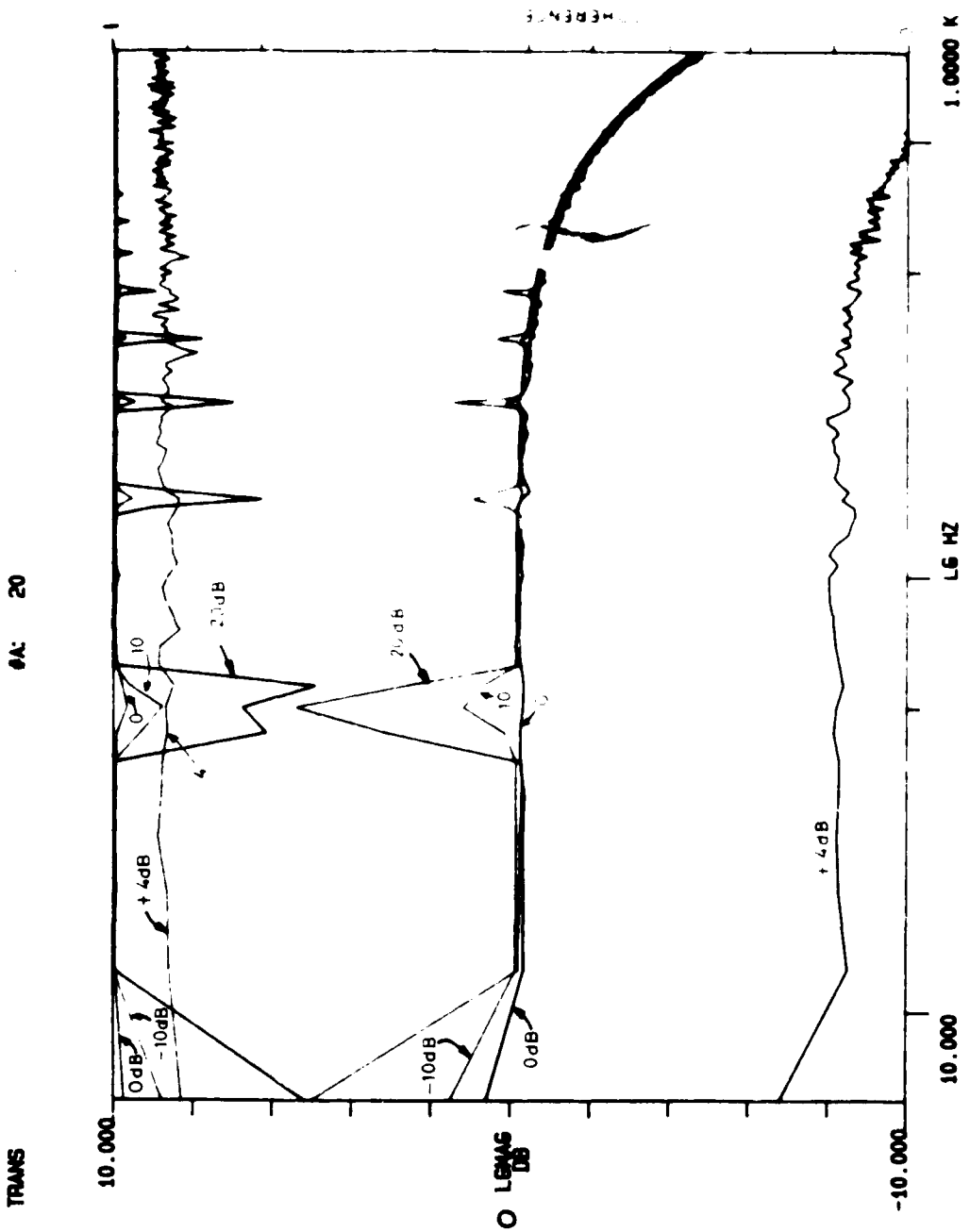

Figure 14. Plots of the coherence (top set of traces) and transfer function amplitude for the TAEC tape recorder channel 1 between the play and replay channels for various recording levels as indicated

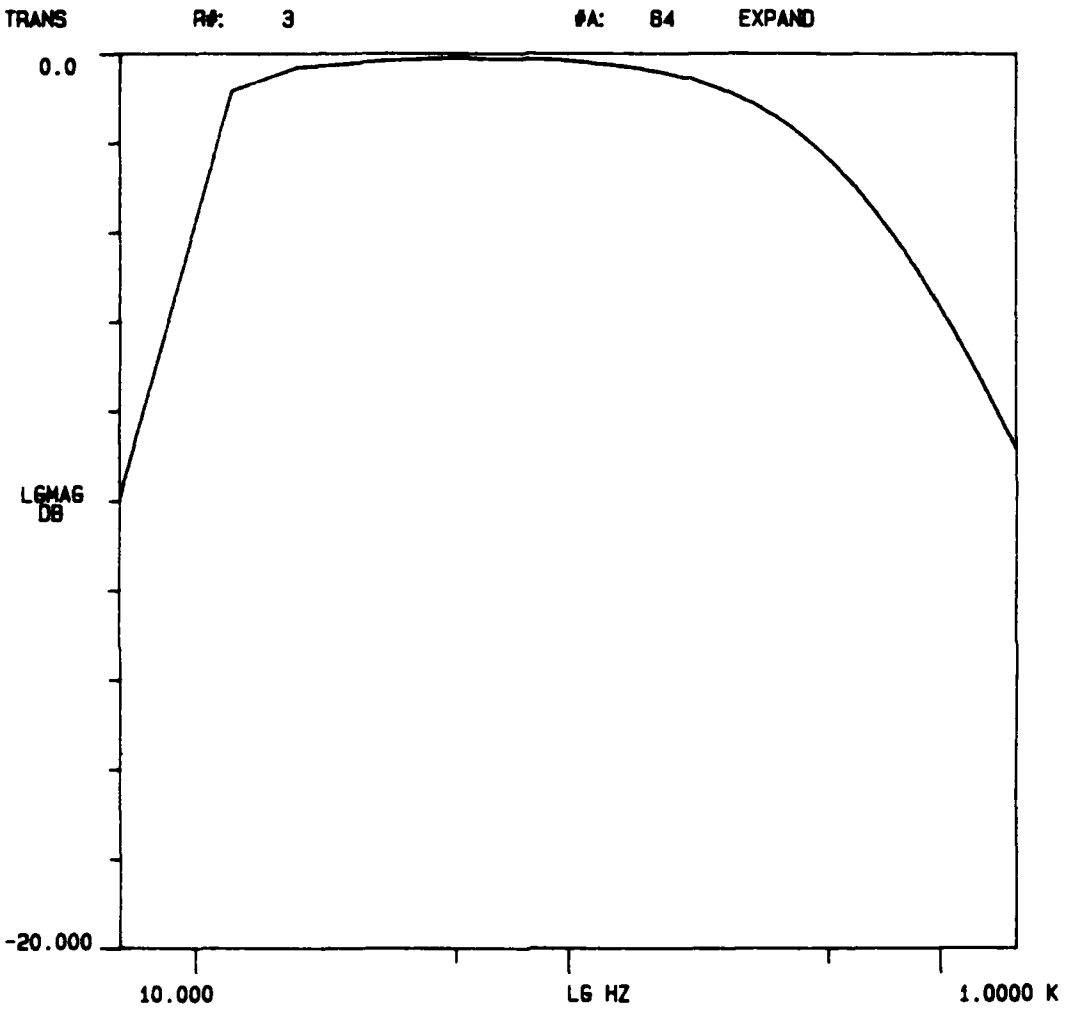

Figure 15. A plot of the transfer function of the signal amplifier used to amplify the signal prior to tape recording. The gain is switched to 0 dB, the gain is within ±0.2 dB at other settings and is an identical shape

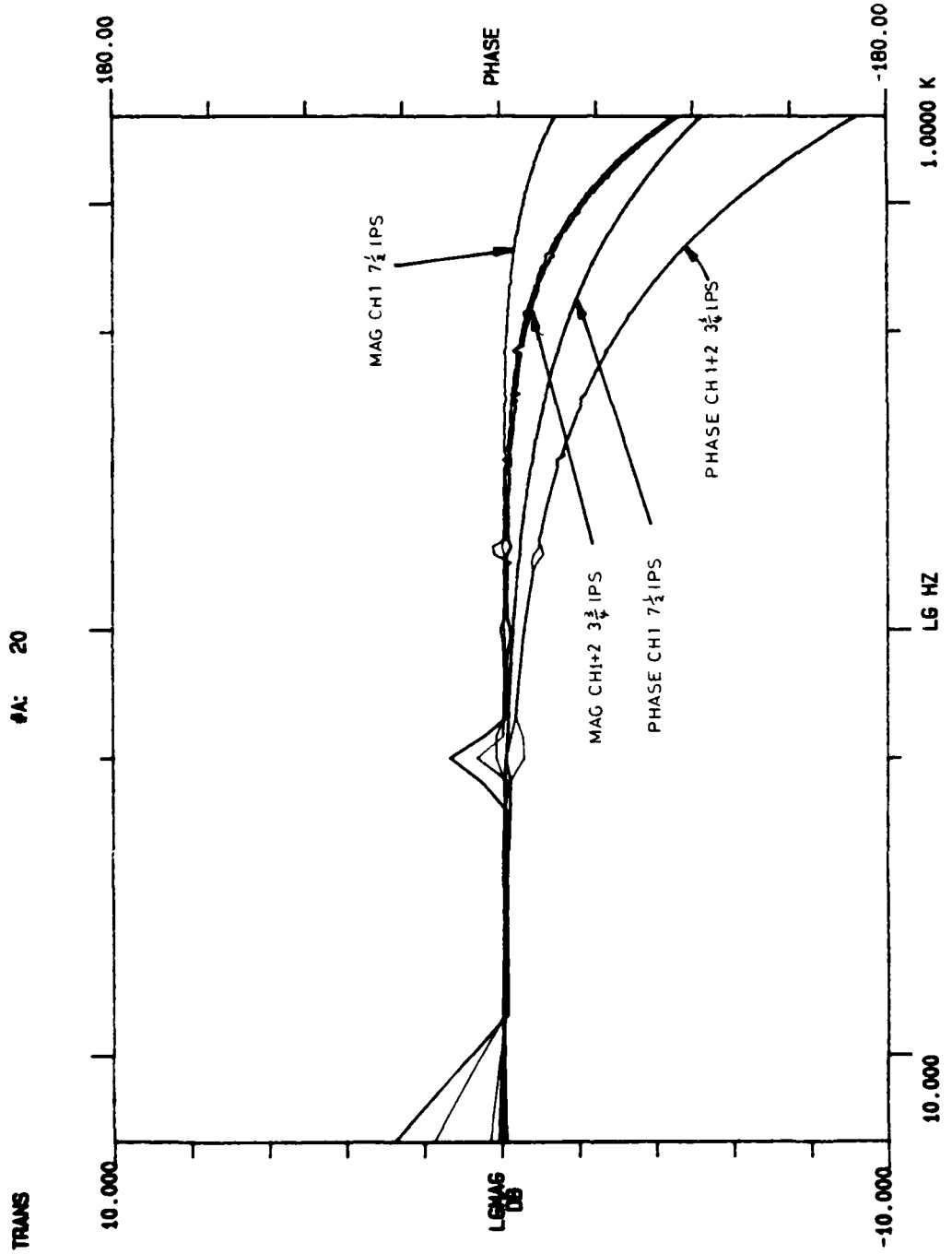

Figure 16. The transfer function between record and replay, channels 1 and 2 at $3\frac{3}{4}$ ip/s and $7\frac{1}{2}$ ip/s tape speeds using TDK AD120 tape

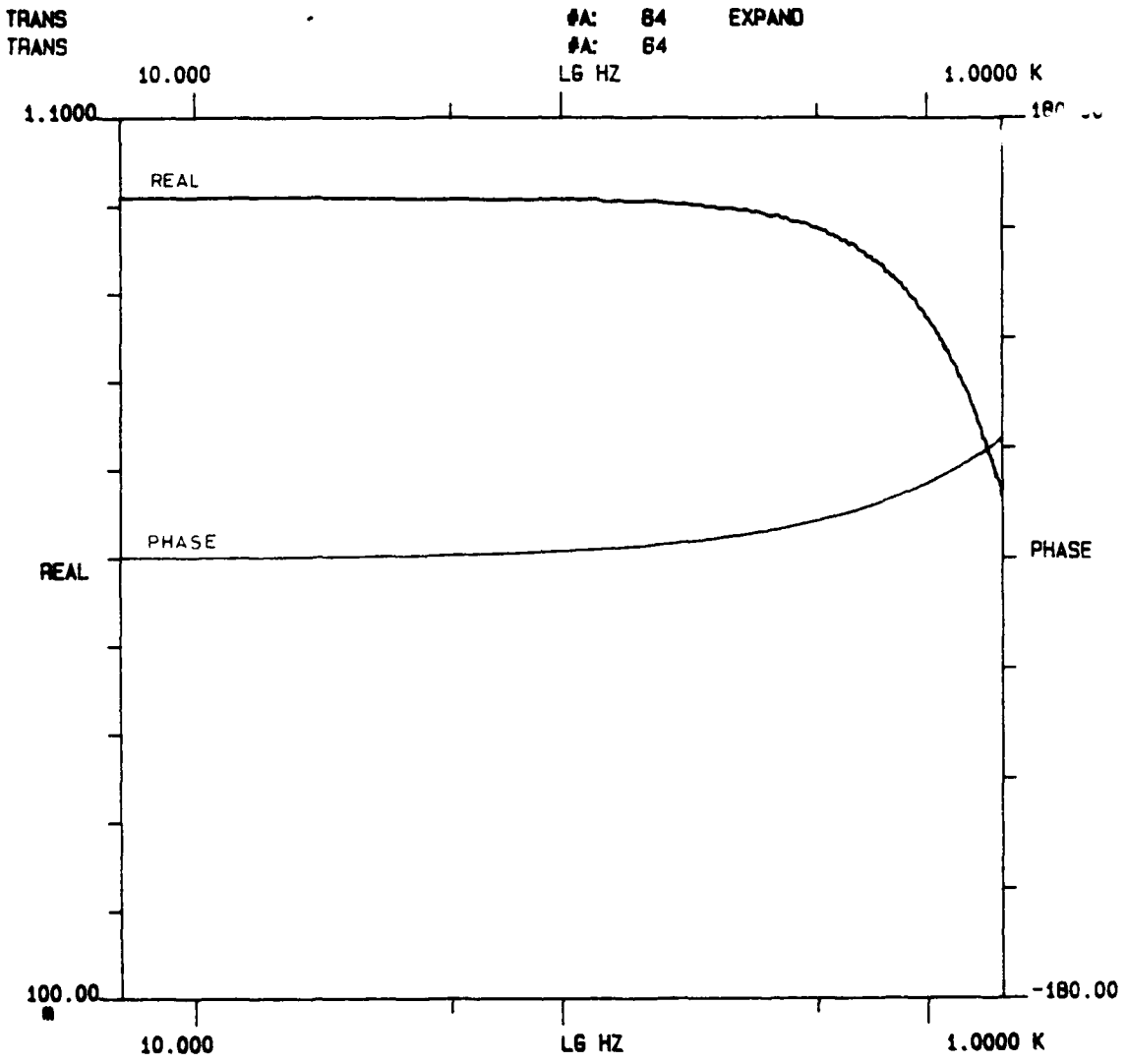

Figure 17. The transfer function between channels 1 and 2 after pseudo-random noise was recorded via one machine and played back on another. The magnitude is indicated by a dotted line

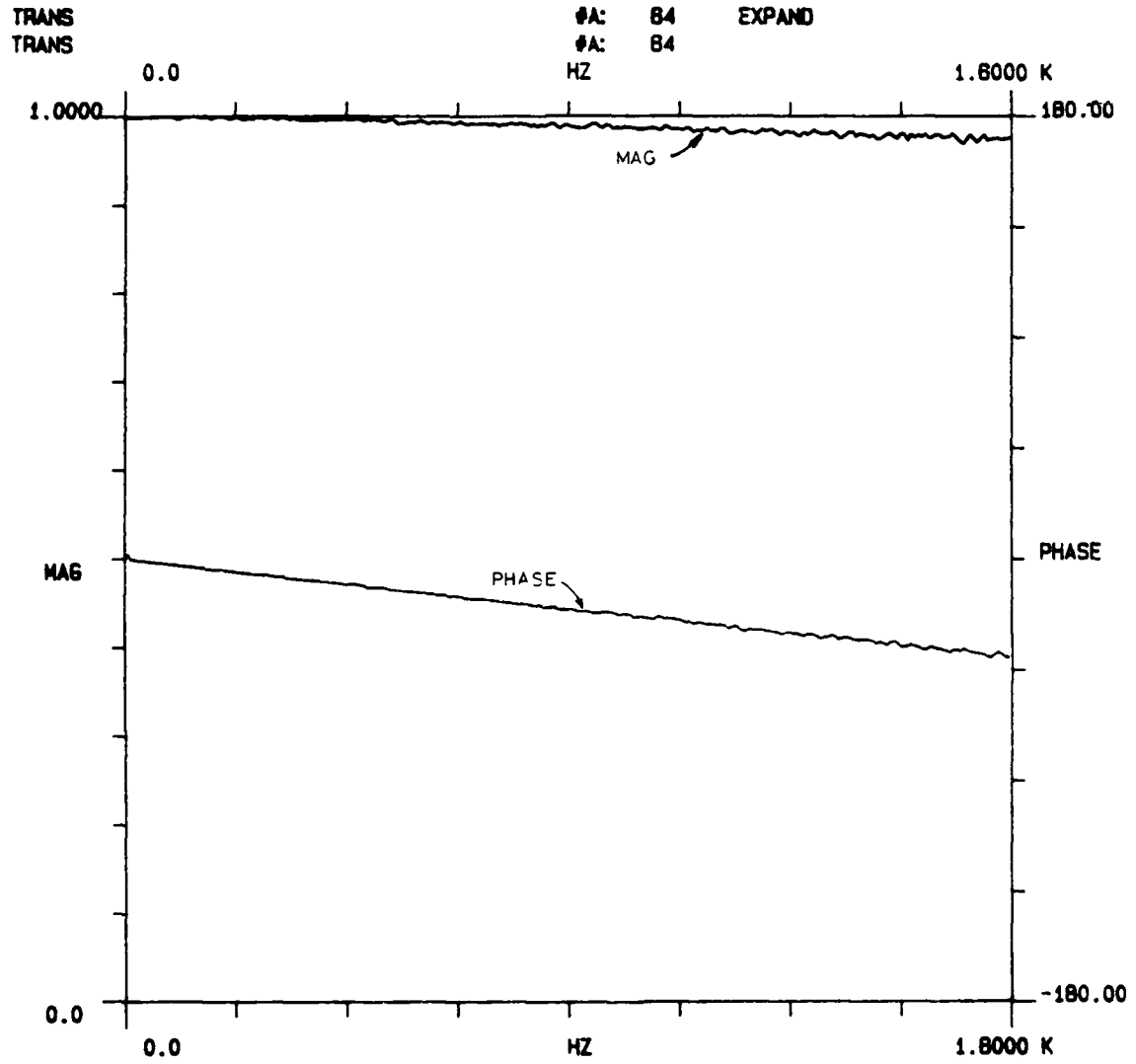

Figure 18. The transfer function between channels 1 and 7 after pseudo-random noise was recorded via one machine and played back on another

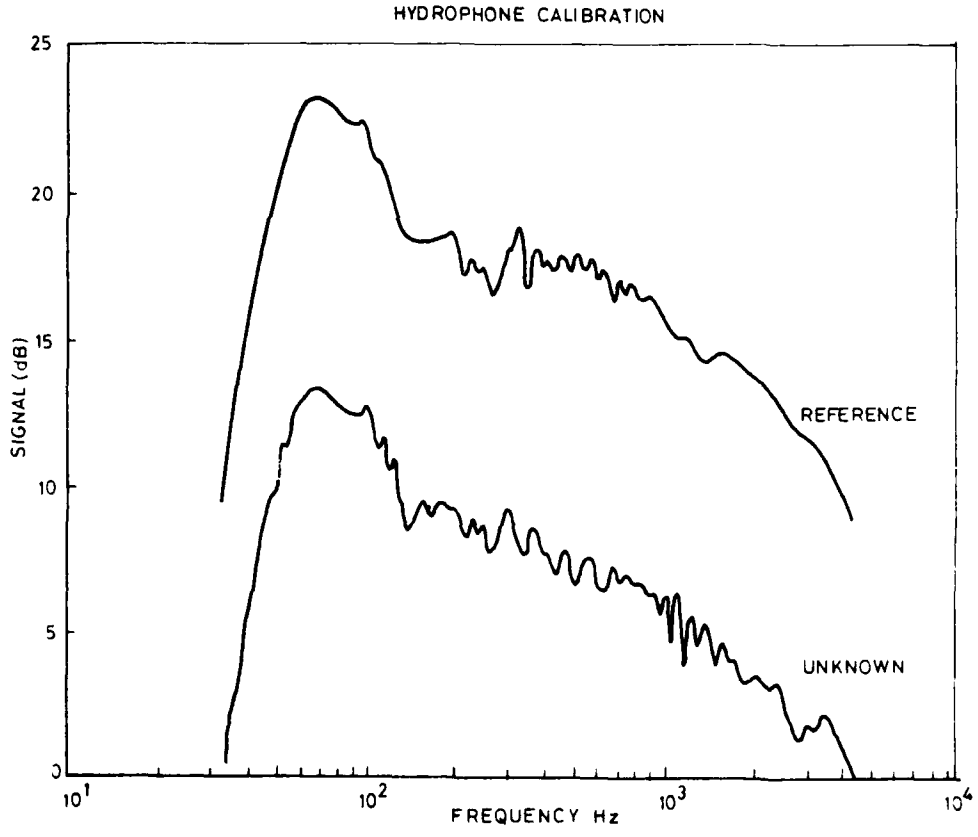

Figure 19. An example of the cross calibration of two hydrophones using the swept frequency method. Only relative signal levels are shown

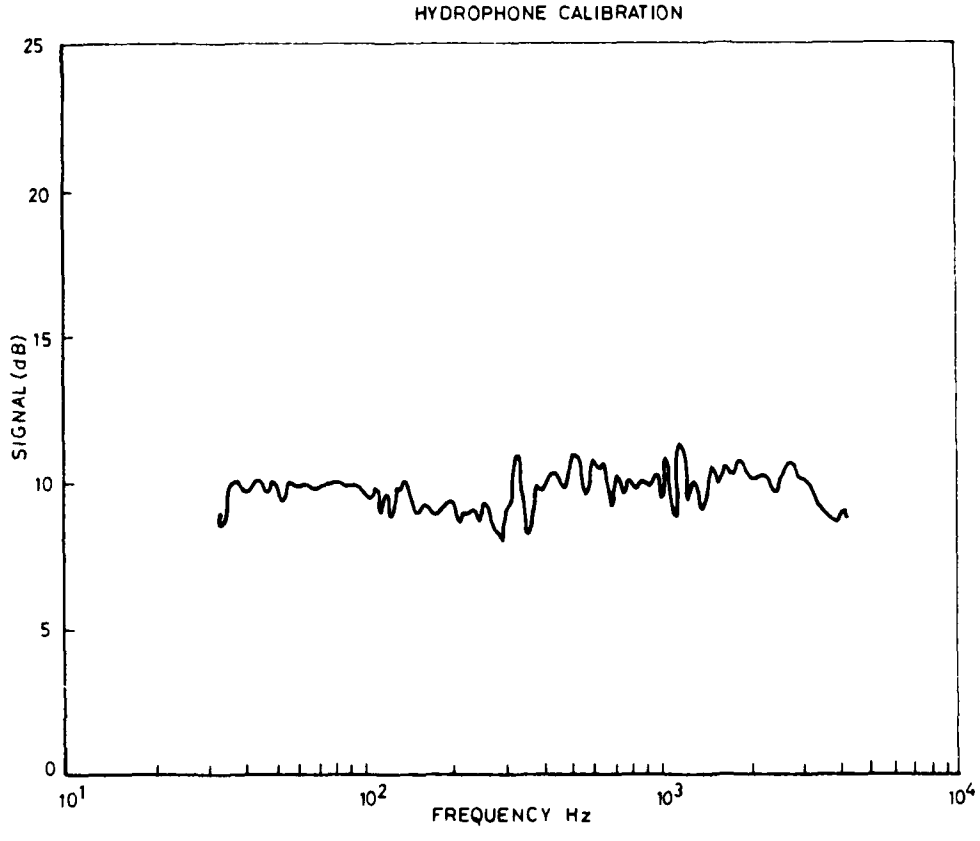

Figure 20. The difference in sensitivity between the two hydrophones plotted on a logarithmic frequency scale. Absolute levels are shown

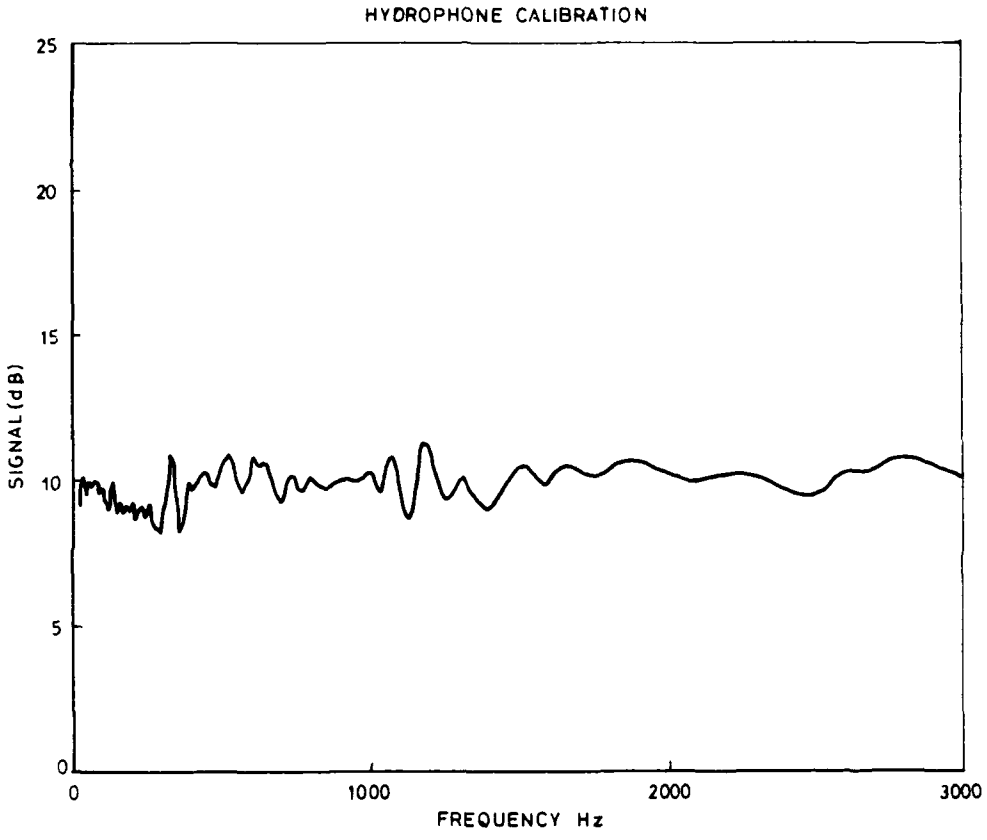

Figure 21. The difference in sensitivity between the two hydrophones plotted on a linear frequency scale. Absolute levels are shown. Note the periodic nature of the fluctuations

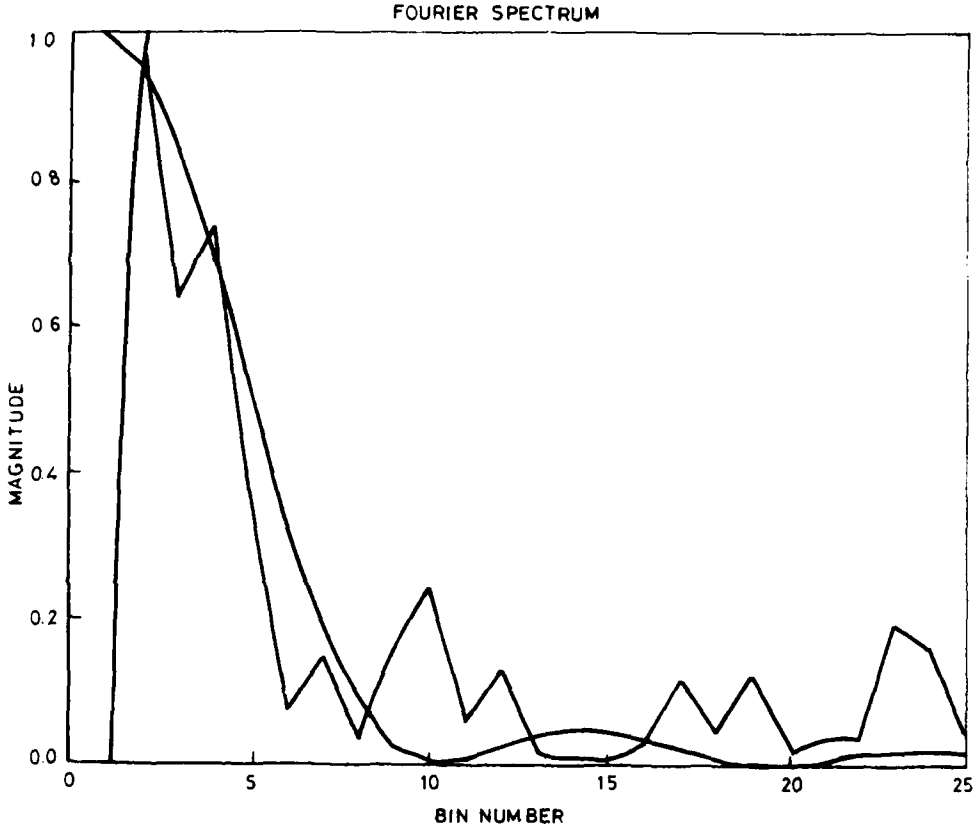

Figure 22. The normalised spectrum of a rectangular window and the difference curve. The window width is chosen so that its minima coincides with some of the higher frequency components

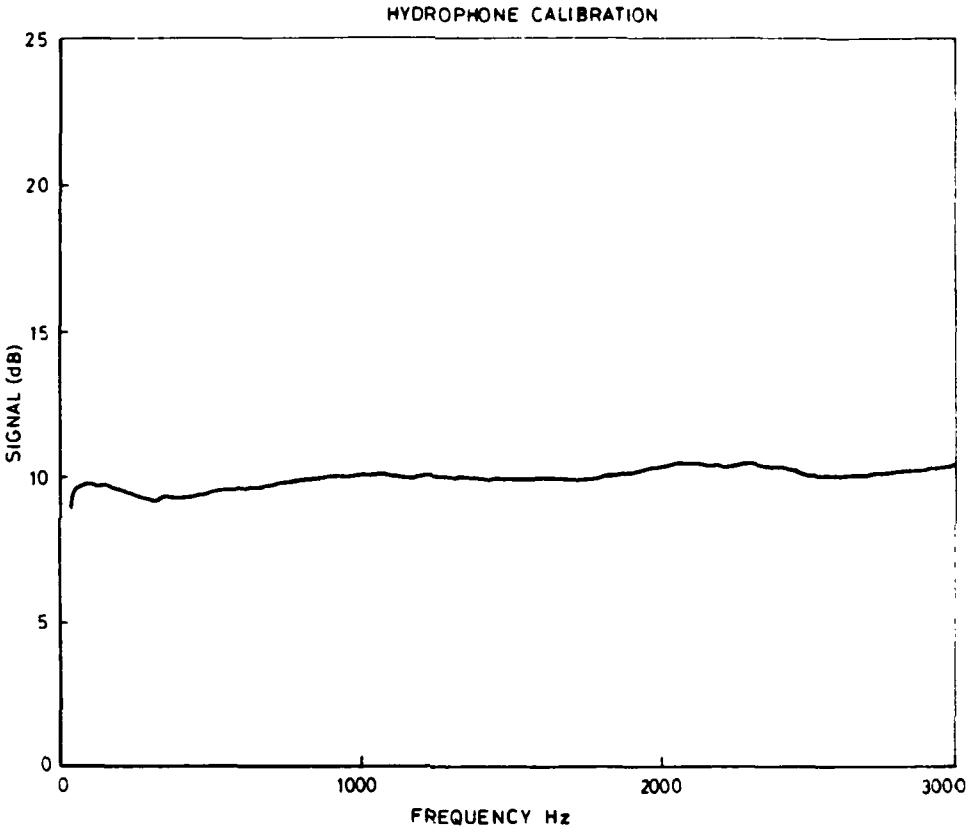

Figure 23. The reconstituted curve after smoothing with the window shown in figure 20

DISTRIBUTION

Copy No.

DEPARTMENT OF DEFENCE

Defence Science and Technology Organisation

Chief Defence Scientist	1
Deputy Chief Defence Scientist	
Controller, External Relations, Projects and Analytical Studies	
Superintendent, Science Programs and Administration	
Defence Science Representative, London	Cnt Sht Only
Counsellor, Defence Science, Washington	Cnt Sht Only

Weapons Systems Research Laboratory

Director, Weapons Systems Research Laboratory	2
Superintendent, Maritime Systems Division	3
Senior Principal Research Scientist, Marine Studies *Composite*	4
Principal Officer, Sea Experiments Group	5
Principal Officer, Underwater Detection Group	6
Principal Officer, Signal Processing and Classification Group	7
Dr A.L. Carpenter, Underwater Detection Group	8
Mr I.H. Cox, Underwater Detection Group	9
Mr J.J.D. Bagley, Sea Experiments Group	10
Author	11

Navy Office

Navy Scientific Adviser	Cnt Sht Only

Army Office

Director General, Army Development (NSO), Russell Offices for ABCA Standardisation Officers	
UK ABCA representative, Canberra	12
US ABCA representative, Canberra	13
Canada ABCA representative, Canberra	14

DOCUMENT CONTROL DATA SHEET

Security classification of this page: UNCLASSIFIED

1 DOCUMENT NUMBERS	2 SECURITY CLASSIFICATION
AR Number: AR-004-117	a. Complete Document: Unclassified
Series Number: WSRL-0383-TR	b. Title in Isolation: Unclassified
Other Numbers:	c. Summary in Isolation: Unclassified

3 TITLE

A COMPARISON OF SWEPT FREQUENCY AND FFT METHODS USED TO CALIBRATE ARRAY TEST MODULES

4 PERSONAL AUTHOR(S):	5 DOCUMENT DATE:
G.B. Gillman	October 1984
	6 6.1 TOTAL NUMBER OF PAGES 39
	6.2 NUMBER OF REFERENCES: 2

7 7.1 CORPORATE AUTHOR(S):	8 REFERENCE NUMBERS
Weapons Systems Research Laboratory	a. Task: DST 80/056
7.2 DOCUMENT SERIES AND NUMBER Weapons Systems Research Laboratory 0383-TR	b. Sponsoring Agency:
	9 COST CODE: 386 BA 326

10 IMPRINT (Publishing organisation)	11 COMPUTER PROGRAM(S) (Title(s) and language(s))
Defence Research Centre Salisbury	

12 RELEASE LIMITATIONS (of the document):

Approved for Public Release

Security classification of this page: UNCLASSIFIED

Security classification of this page: UNCLASSIFIED

13 ANNOUNCEMENT LIMITATIONS (of the information on these pages):

No limitation

14 DESCRIPTORS:

a. EJC Thesaurus Terms

b. Non-Thesaurus Terms

15 COSATI CODES:

16 SUMMARY OR ABSTRACT:
(if this is security classified, the announcement of this report will be similarly classified)

A description is given of swept frequency and FFT methods used to calibrate array test modules. The FFT method is shown to give sensitivity versus frequency plots with relative ease and known accuracy. The swept frequency method is capable of giving similar results but only after operator interpretation of the mean of fluctuating signals and calculations on a point to point basis. A digital filtering method is briefly described which can be used to process the signals obtained in swept frequency calibration obviating the need for operator interpretation. The accuracy of the FFT method is discussed and an overall accuracy figure is obtained for the derived sensitivity of the test array. A summary of the FFT method is given as a guide for future hydrophone calibration experiments.

Security classification of this page: UNCLASSIFIED

The official documents produced by the Laboratories of the Defence Research Centre Salisbury are issued in one of five categories: Reports, Technical Reports, Technical Memoranda, Manuals and Specifications. The purpose of the latter two categories is self-evident, with the other three categories being used for the following purposes:

Reports	:	documents prepared for managerial purposes.
Technical Reports	:	records of scientific and technical work of a permanent value intended for other scientists and technologists working in the field.
Technical Memoranda	:	intended primarily for disseminating information within the DSTO. They are usually tentative in nature and reflect the personal views of the author.

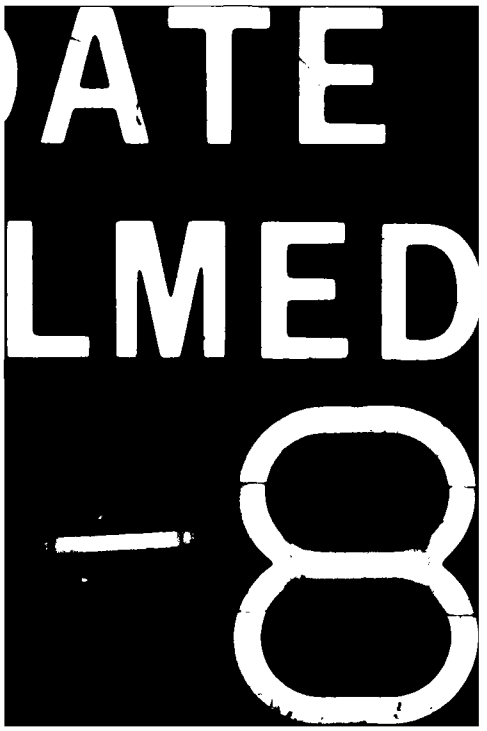
ATE
LMED
8